博士論文

論文題目　An Experimental Study on Chlorine Partitioning in the Earth during Core Formation

(核形成期の地球における塩素分配に関する実験的研究)

氏　名　　桑原　秀治

An Experimental Study on Chlorine Partitioning in the Earth during Core Formation

(核形成期の地球における塩素分配に関する実験的研究)

by

Hideharu Kuwahara

A thesis submitted to

the Department of Complexity Sciences and Engineering

In partial fulfillment of the requirements

for the degree of Doctor of Philosophy

The University of Tokyo

Kashiwa, Chiba

Acknowledgements

I would like to thank my adviser, Seiji Sugita, for academic freedom to explore ideas and financial supports throughout my graduate study, though my initial ideas were probably very immature and could have been a little bit crazy. This gave me a chance to think thoroughly about my own research ideas and mature them. I would like to thank the people who helped the experiments and analyses. Takehiko Yagi, Hirotada Gotou, and Daisuke Hamane gave me the opportunity for conducting high pressure experiments described in Chapter 2. They also gave me helpful comments both on experiments and analyses. Asuka Yamaguchi and Nobuhiro Ogawa helped the electron microprobe analyses. Yuji Sano and Naoto Takahata helped the secondly ion mass spectrometry analyses. This study would not have been completed without their help. I would like to express my gratitude to the Visiting Researcher's Program of Geodynamics Research Center (GRC), Ehime University. In particular, I would greatly thank Tetsuo Irifune, Toru Inoue, Toru Shinmei, Masayuki Nishi, Vincenzo Stagno, and Steeve Gréaux for their technical assistances and constructive comments which greatly improved the study described in Chapters 2 and 3. Discussion with them was always insightful and gave me an opportunity for conceiving ideas on the next challenge. I thank the members of research groups of the University of Tokyo in the past and present. I also thank all of the people who always encouraged me when I wanted to get away from the University of Tokyo culture. Finally, I am grateful to the thesis advisory committee (alphabetical order): Hiroyuki Kagi, Kei Kurita, Koichiro Saiki, Seiji Sugita, and Eiichi Tajika. Their helpful comments improved this study.

Abstract

The absolute and relative abundances of Earth's volatile elements are geochemical tracers for understanding the origin of Earth's atmosphere and ocean. Specifically, core-mantle differentiation may have caused the depletion of siderophile volatiles, whereas Atmospheric loss may have caused the depletion of lithophile volatiles. Although the partitioning behavior of volatiles between core and mantle during planetary differentiation is crucial for understanding the formation of Earth's atmosphere and ocean, the partitioning of volatiles between core and mantle has not been understood well.

In this thesis, we focus on terrestrial missing chlorine problem. Chlorine in the accessible part of the Earth is depleted relative to other elements with similar volatility. Such observation requires the presence of hidden chlorine-rich reservoirs in the deep Earth's interior or the loss of primordial chlorine-rich reservoir to space. In order to investigate the presence of hidden chlorine-rich reservoirs in the deep Earth's interior, we have experimentally determined chlorine partitioning among metallic liquids, silicate minerals, and silicate melts.

In Chapter 1, we discuss the background and the purpose of this study. In Chapter 2, we experimentally investigated the metal-silicate partitioning of chlorine to examine the incorporation of chlorine into the core. Our experimental results combined with thermodynamic considerations indicate that the partition coefficients of chlorine between metallic liquids and silicate melts at the relevant pressure-temperature conditions of core-mantle differentiation are not above the unity. The result indicate that chlorine is very difficult to deplete from the bulk silicate Earth by dissolution to the metallic core during early differentiation phase. Consequently, terrestrial chlorine may have been lost from the Earth and/or trapped in the deep mantle during the late accretion stage. In Chapter 3,

we experimentally determined silicate mineral-melt partitioning of chlorine at the transition zone and lower mantle conditions. Our results show that chlorine is highly incompatible in deep mantle minerals. Because previous studies have shown that chlorine is highly incompatible to silicate minerals that occurs in the upper mantle, this experimental result strongly suggests that chlorine would have been concentrated in the residual silicate melts during magma ocean solidification at all depths. In Chapter 4, we discuss implications of our experimental results for the origin of terrestrial missing chlorine. Our experimental results indicate that chlorine supplied to the Earth would have been concentrated to the crust, similarly to other incompatible lithophile and moderately volatile elements, such as potassium and zinc. However, these elements are not as deplete as chlorine. A major difference between chlorine and other incompatible lithophile elements is solubility to water. Chlorine has much higher solubility than other elements, it would be concentrated in hydrosphere. Given that the Cl/K and Cl/Zn ratios of the Earth are lower than any types of chondrites, chlorine would have been lost to space possibly via an erosion of primordial hydrosphere during the main-accretion phase. In Chapter 5, we summarize the study and conclude that terrestrial missing chlorine may require an extensive loss of primordial chlorine-rich reservoir to space, probably an oceanic loss event. If so, the chlorine abundances of terrestrial planets may be used as record for an oceanic loss event. Such a geochemical indicator is important for understanding the origin of atmosphere and ocean of the Earth.

Contents

List of Tables

List of Figures

1. General Introduction

Elucidating the partitioning of volatile elements during the formation of terrestrial planets is a key to understanding the origins of terrestrial planetary atmospheres. The formation of processes of terrestrial planetary atmospheres have been inferred from the absolute and relative abundances of volatile elements in the accessible part of terrestrial planets (e.g., Anders and Owen, 1977; Broadhurst et al., 1992; Kuramoto and Matsui, 1996; Hirschmann and Dasgupta, 2009; Shcheka and Keppler, 2012; Marty, 2012; Halliday, 2013; Hirschmann, 2016), because siderophile or incompatible lithophile volatile elements are generally depleted as a consequence of either the incorporation into the core or escape to space. In the following sections, we briefly discuss 1) theoretical predictions and geochemical evidences on planetary differentiation, 2) the abundance pattern of volatile elements on Earth, and 3) the purpose of this study.

1.1. Magma ocean and core formation

When protoplanets became larger than 0.1 Earth's mass, primordial atmospheres would have formed by capturing solar nebula (e.g., Hayashi et al., 1979) or impact degassing of volatiles from accreting materials (e.g., Abe and Matsui, 1985; Matsui and Abe, 1986a; 1986b). The greenhouse effect of such a gravitationally captured atmosphere which was probably composed mainly of H_2 and H_2O, would have retained the surface temperature above solidus (e.g., Hayashi et al., 1979; Abe and Matusi 1985; Matsui and Abe, 1986a; 1986b). In addition, theoretical studies have indicated that terrestrial planets would have experienced a giant impact during the end of accretion (e.g., Chambers et al., 1996; Chambers and Wetherill, 1998). Such an energetic impact would have molten the mantle of terrestrial planets (e.g., Tonks and Melosh, 1992; 1993; Nakajima and Stevenson,

2015). It is therefore widely accepted that terrestrial planets, such as Venus, Earth, and Mars, would have been at least once almost completely molten due to the greenhouse effect of primordial atmospheres and an energetic impact during planetary accretion phases.

The magma ocean hypothesis has been supported by many lines of geochemical evidence. The best candidate for the presence of a magma ocean is probably the abundance pattern of siderophile (iron-loving) elements in terrestrial mantle (e.g., Ringwood, 1966; Li and Agee, 1996; Wood et al., 2006). The partitioning behavior of siderophile elements between metallic liquids and silicate melts is mainly controlled by pressure and temperature. Thus, the depletion pattern of siderophile elements in the mantle would reflect the mean pressure and temperature condition of the core-mantle segregation. Previous studies have suggested that the base of a magma ocean at which the metal-silicate partitioning of elements achieves equilibrium may have been deeper than 400 km (e.g., Li and Agee, 1996; Wade and Wood, 2005: Wood et al., 2006; Siebert et al., 2011; 2012). Although volatiles would have mainly degassed into atmosphere, some volatiles dissolved in a magma ocean would also have partitioned between core and mantle (e.g., Okuchi, 1997; Roskosz et al., 2013; Dasgupta et al., 2013; Chi et al., 2014). Thus, some siderophile volatile elements are more depleted than other volatile elements.

1.2.Atmospheric loss

During the formation of terrestrial planets, there are mainly two processes for removing the primordial atmosphere and ocean of terrestrial planets to space: hydrodynamic escape and impact erosion (e.g., Kasting and Pollack, 1983; Melosh and Vickery, 1989; Pepin, 1991; Genda and Abe, 2005; Shuvalov, 2009; Schlichting et al., 2015). The former case

is caused by the escape of a hydrogen-rich atmosphere driven by the solar extreme ultraviolet irradiation from the young sun. For the latter case, numerical simulations have shown that a giant impact efficiently erodes a pre-existence atmosphere when protoplanets had an ocean (Genda and Abe, 2005). Based on theoretical studies, timescales for water condensation in a steam atmosphere are shorter than the typical interval of time between giant impacts if protoplanets were located beyond 1 AU (Lebrun et al., 2013). Moreover, almost all of water in a steam atmosphere of the Earth may have been retained during magma ocean solidification (Hamano et al., 2013). Thus, the proto-Earth may have been covered with an ocean before a giant impact if accreting planetesimals contained water. These studies suggest that the loss of primordial Earth's atmosphere by a giant impact would have occurred. In addition, a high-velocity impact of small planetesimals may also have efficiently eroded the Earth's atmosphere and ocean (e.g., Shuvalov, 2009; Schlichting et al., 2015). These theoretical studies have suggested that the primordial atmosphere and ocean of terrestrial planets may have extensively lost to space during the accretion phase.

1.3. Late addition of volatiles after core formation

Highly siderophile elements in Earth's mantle are much more abundant than the expected values from their extremely high metal-silicate partition coefficients (e.g., Kimura et al., 1974). The problem is now generally interpreted as a natural consequence of late-accreting materials after the core-mantle differentiation (e.g., Chou, 1978). Given that other terrestrial planets (i.e., Moon, Mars, and Vesta) also shows the excess of highly sideophile elements in mantles (e.g., Day et al., 2007; Dale et al., 2012; Day et al., 2012), the late addition of primitive materials after the formation of terrestrial planets would

have been a common phenomenon in our solar system. Based on theoretical studies, the late-accreting materials would have come from the region beyond the snow line at which H_2O ice becomes stable (e.g., Raymond et al., 2004; 2005; O'Brien et al., 2014). In addition, the abundance pattern of chalcophile elements which become highly siderophile at high pressure and temperature conditions (e.g., Rose-Weston et al., 2009; Boujibar et al., 2014) in Earth's mantle also requires the late addition of a modest amount of CI-like materials (Wang and Becker, 2013). This indicates that the late addition of volatiles was likely. Here it is noted that the impact of late-accreting materials may have eroded a pre-existence atmosphere. Although the role of impact delivery and erosion of volatiles is still poorly understood, the early atmospheres of terrestrial planets during heavy bombardment may have been replaced (e.g., Hamano and Abe, 2010; de Niem et al., 2012). Taken together, the absolute and relative abundances of volatile elements at the planetary surface would have been controlled by 1) partitioning between core, mantle, and atmosphere, 2) the loss of primordial atmosphere and ocean, and 3) the late addition of volatiles after the formation of terrestrial planets.

1.4. The absolute and relative abundances of terrestrial volatiles

In comparison with the solar composition, noble gases in the atmosphere of terrestrial planets are significantly depleted relative to other volatile elements, such as H, C, and N (e.g., Brown, 1949; Halliday, 2013). More specifically, the Ne/N ratio of the solar composition is approximately the unity, whereas Ne in the Earth's atmosphere is several orders of magnitude lower than N. Given that the atomic mass of Ne is very similar to N, the mass fractionation during atmospheric escape would have been limited. Such observations indicate that terrestrial planetary atmospheres were not originated from the

solar nebula. In contrast, the abundance pattern of volatile elements on terrestrial planets is broadly chondritic (e.g., Marty, 2012; Halliday, 2013). Thus, the atmosphere of terrestrial planets would have been formed from the degassing of volatiles from chondritic materials.

A canonical model for the volatile accretion of terrestrial planets is the late addition of volatile-rich materials, such as CI chondrites, to the primordial Earth (e.g., Albarède, 2009). Indeed, the abundance pattern of volatiles and the isotopic ratios of H, C, and N of the Earth are broadly CI chondritic (e.g., Marty, 2012; Alexander et al., 2012). However, some previous studies have pointed out that the late addition of volatile-rich chondrites to dry proto-Earth cannot explain both on the absolute and relative abundances of terrestrial volatiles (e.g., Halliday, 2013). Thus, it has been suggested that terrestrial volatiles have experienced fractionations after the delivery of volatiles (e.g., Tolstikhin and O'Nions, 1994; Kuramoto and Matsui, 1996; Hirschmann and Dasgupta, 2009; Shcheka and Keppler, 2012; Halliday, 2013; Tucker and Mukhopadhyay, 2014).

1.4.1. Noble gases

The abundance pattern of noble gases which are generally insoluble in a magma ocean has been the powerful tracer for understanding the origin and evolution of atmospheres. For example, the Xe/H and Xe/Ar ratios of the Earth are lower than any types of chondrites (Anders and Owen, 1977; Pepin, 1992; Pepin and Porcelli, 2002; Dauphas and Morbidelli, 2014), suggesting that terrestrial xenon would have been selectively scavenged. Because xenon has the lowest solubility in silicate melts and incompatibility with minerals among noble gases, the earliest Earth's atmosphere may have been rich in xenon (Tolstikhin and O'Nions, 1994; Shcheka and Keppler, 2012). If this is the case, the

loss of primordial atmosphere during the accretion phase can explain terrestrial missing xenon. In contrast, it has been reported that the isotopic ratios of ancient atmospheric Xe trapped in ancient sedimentary rocks were lighter and more chondritic than present values (Pujol et al., 2011). The observation indicates that terrestrial Xe may have been selectively lost to space after the formation of Earth's atmosphere (Pujol et al., 2011; Halliday, 2013).

1.4.2. H, C, and N

The C/H and N/H ratios of the Earth are lower than any types of chondrites (Hirschmann and Dasgpta, 2009; Halliday, 2013; Tucker and Mukhopadhyay, 2014). Based on the estimate of the abundances of terrestrial volatiles, the depletions of C and N relative to H are ordered as N > C (Marty, 2012; Halliday, 2013). These observations indicate that the fractionation of C/H and N/H ratios occurred during planetary accretion. The C/H ratios of the Earth may be achieved by either partitioning of C into the core or a loss of primordial atmospheres (Hirschmann and Dasgpta, 2009; Halliday, 2013; Tucker and Mukhopadhyay, 2014). For the N/H ratios of the Earth, Marty (2012) and Roskosz et al. (2013) have argued that the depletion of N was achieved by partitioning of N into the core due to the siderophile behavior of N. However, Tucker and Mukhopadhyay (2014) have argued that the incorporation of N into the core is unlikely because the metal-silicate partition coefficient of carbon is generally much higher than that of nitrogen (e.g., Dasgupta et al., 2013; Chi et al., 2014). Given that terrestrial nitrogen is more depleted than carbon, the N/H ratios of the Earth may reflect the selective loss of a primordial atmosphere (Tucker and Mukhopadhyay, 2014).

Although such geochemical inferences of atmospheric loss episodes during the accretion phase provide clues for understanding the origin of Earth's atmosphere and

ocean, the origin of the non-chondritic pattern of H/C/N on Earth is still controversial. For example, terrestrial nitrogen may have been retained in the deep Earth's mantle if ammonium ion was the dominant specie of nitrogen in the mantle (e.g., Li et al., 2013).

1.4.3. Halogens

Previous studies have indicated that the absolute and relative abundances of noble gases and H, C, and N on Earth are explained by partitioning between core, mantle, and atmosphere, and/or atmospheric loss during the accretion phase. In order to further constrain the origin of Earth's atmosphere and ocean, other depleted volatile elements should also be investigated.

Heavy halogens (i.e., Cl, Br, I), volatile and incompatible elements, may also provide unique information on the formation of terrestrial atmosphere and ocean. Heavy halogens of the Earth are depleted compared to chondrites and other volatile elements, such as potassium and zinc (Campbell and O'Neill, 2012; Sharp and Draper, 2013). Thus, the depletion of terrestrial halogens is thought to be caused by either the incorporation into the core or a loss of atmosphere and/or ocean (e.g., McDonough, 2003; Sharp and Draper, 2013). If the metal-silicate partition coefficients of heavy halogens are higher than the required values for explaining the depletions in the mantle, chemical characteristics of terrestrial halogens in the mantle may be a fingerprint of the late-accreting materials. In contrast, if the partitioning of chlorine into the core was limited, an extensive loss of primordial hydrosphere may be required because chlorine is strongly partitioned into fluid phase at low-pressure conditions (e.g., Fabbrizio et al., 2013a; 2013b). Thus, the heavy halogens may provide clues to the source of late-accreting materials or the formation process of terrestrial atmosphere and ocean. In order to constrain the origin of missing

heavy halogens, the partition coefficients among metallic liquids, silicate liquids, and minerals at the base of a magma ocean are needed. However, the partitioning behavior of heavy halogens in a magma ocean has been still poorly constrained.

1.5. The purpose of this study

In this study, we focus on the partitioning behavior of chlorine during the core-mantle differentiation. This is because observational constraints on terrestrial chlorine are more abundant than other heavy halogens. In addition, chlorine has stable isotopes. Thus, the isotopic compositions of terrestrial chlorine also provide constraints on mechanisms for removing chlorine. In Chapter 2, we have experimentally investigated the partitioning of chlorine between metallic liquids and silicate melts to assess the depletion of terrestrial chlorine by partitioning into the core. In Chapter 3, we have experimentally investigated the partitioning of chlorine between silicate melts and minerals at the deep mantle conditions to assess the retention of chlorine in the deep mantle during magma ocean solidification. In Chapter 4, we discuss implications of experimental results for the origin of terrestrial missing chlorine. In Chapter 5, we summarize our study.

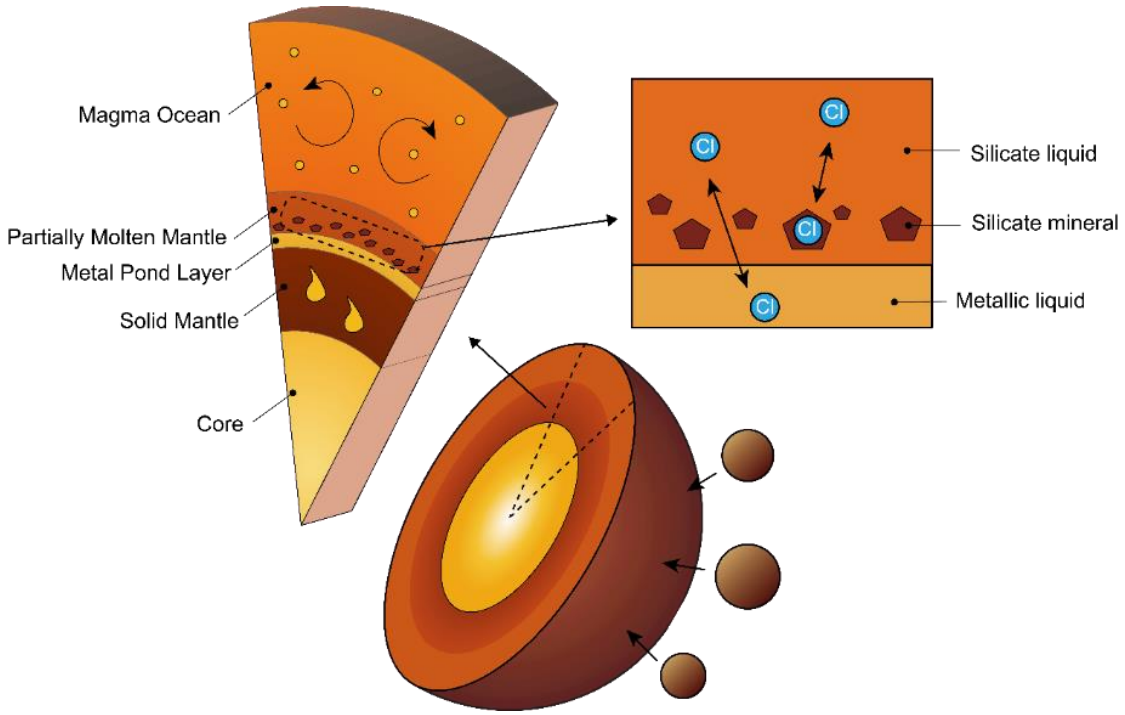

Figure 1.1. Schematic view of the scope of this study. In this study, we focus on chlorine partitioning among metallic liquids, silicate liquids, and silicate minerals at the base of magma oceans.

2. Partitioning of chlorine between metal and silicate: Implications for the origin of terrestrial missing chlorine.

2.1. Introduction

Heavy halogens (i.e., Cl, Br, I), incompatible and highly volatile elements, in the bulk silicate Earth (BSE) are depleted relative to the predicted values from their volatilities and chondrites (McDonough and Sun, 1995; Campbell and O'Neill, 2012; Sharp and Draper, 2013) (Fig. 2.1). Such observations require that halogen reservoir have lost due to dynamic accretion processes. Previous studies have proposed two possible scenarios for explaining the origin of terrestrial missing heavy halogens: The incorporation into the core and an extensive loss of primordial hydrosphere (McDonough and Sun, 1995; Campbell and O'Neill, 2012; Sharp and Draper, 2013). If the former case is correct, the abundance pattern of heavy halogens in Earth's mantle would be a fingerprint of the late veneer, whereas the latter case provides clues to the origin of the Earth's atmosphere and ocean. Therefore, elucidating the origin of terrestrial missing halogens is a key constraint on the late accretion of the Earth, possibly Venus and Mars.

Previous studies have indicated that iodine is a siderophile element (Armytage et al., 2013), whereas chlorine is a slightly chalchophile and a lithophile element (Mungall and Brenan, 2003; Sharp and Draper, 2013). However, the core-mantle partitioning of heavy halogens has been still poorly constrained due to a lack of experimental data on the effects of pressure, temperature, and compositions.

Among heavy halogens, chlorine has stable isotopes and is the most abundant on the

Earth, providing better constraints on the mechanism of missing heavy halogens from the observational point of view. Thus, in this study, we focus on the origin of terrestrial missing chlorine. More specifically, we experimentally investigate the possibility of the incorporation of chlorine into the core during planetary differentiation. In the following § 2.3, § 2.4, and § 2.5, we first describe our experimental and analytical procedures, in § 2.6, we show the effects of pressure, temperature, and metallic compositions on the metal-silicate partitioning of chlorine, in § 2.7 and § 2.8, we discuss the origin of terrestrial missing chlorine inferred from our experimental constraints, and in § 2.9, we summarize our study.

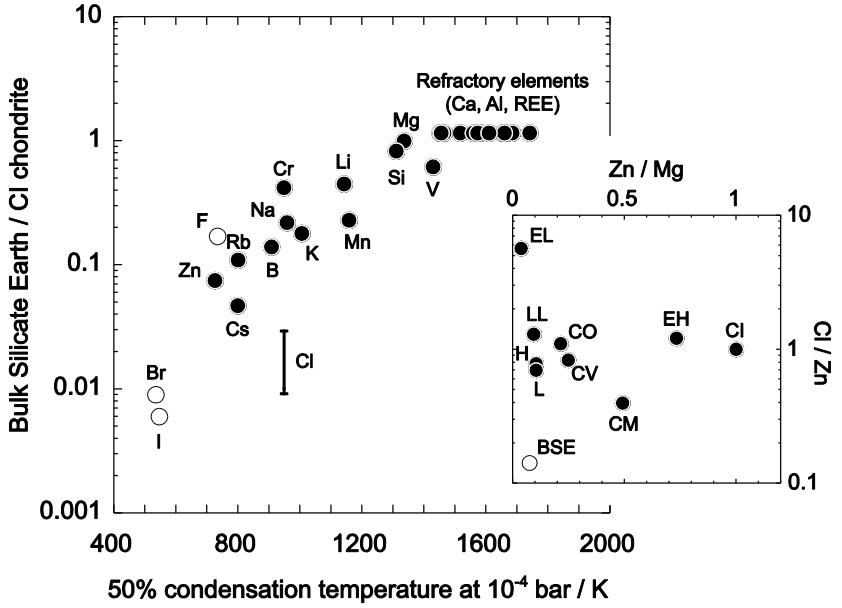

Figure 2.1. The depletion pattern of heavy halogens and lithophile elements of the BSE. The abundances of each element normalized to CI chondrites and Mg are plotted against nebular condensation temperature (data from McDonough and Sun, 1995; Lodders, 2003). The solid line indicates the range of chlorine abundances of the BSE (data from Sharp and Draper, 2013 and references therein). The positive slope in the lithophile elements is the volatile depletion trend, which may be a consequence of volatility-dependent fractionations caused by a mantle-stipping impact during Earth's accretion (e.g., Boujibar et al., 2015). Terrestrial chlorine is anomalously depleted relative to a volatile depletion trend, suggesting that terrestrial chlorine reservoir have been lost to space and/or deep interior of the Earth.

2.2. Parameterization of the metal-silicate partitioning of elements

The metal-silicate partitioning of chlorine is described by the following equation using the equilibrium constant:

$$K_{\mathrm{eq}} = \frac{[\gamma]_{\mathrm{Cl}}^{\mathrm{met}}[X]_{\mathrm{Cl}}^{\mathrm{met}}}{[\gamma]_{\mathrm{Cl}}^{\mathrm{sil}}[X]_{\mathrm{Cl}}^{\mathrm{sil}}} \tag{2.1}$$

Here, K_{eq}, $[\gamma]_{\mathrm{Cl}}^{\mathrm{met}}$, $[\gamma]_{\mathrm{Cl}}^{\mathrm{sil}}$, $[X]_{\mathrm{Cl}}^{\mathrm{met}}$, and $[X]_{\mathrm{Cl}}^{\mathrm{sil}}$ are the equilibrium constant for metal-silicate partition reaction of chlorine, the activity coefficients and the mole fractions of chlorine in metal and silicate phase, respectively. Based on the thermodynamic relation, the equilibrium constant is given as a function of pressure and temperature in the following equation:

$$\ln K_{\mathrm{eq}} = -\frac{\Delta H}{RT} + \frac{\Delta S}{R} - \frac{P\Delta V}{RT} \tag{2.2}$$

Here, R, P, T, ΔH, ΔS, and ΔV are the gas constant, pressure, temperature, the changes in enthalpy, entropy, and volume of the partition reaction of chlorine, respectively. Mole fraction can be recast as mass concentration. Thus, equation (2.2) can also be recast as

$$\log D_{Cl}^{\mathrm{met/sil}} = \log \frac{[C]_{\mathrm{Cl}}^{\mathrm{met}}}{[C]_{\mathrm{Cl}}^{\mathrm{sil}}} = a + \frac{b}{T} + c\frac{P}{T} \tag{2.3}$$

where, $D_{Cl}^{\mathrm{met/sil}}$, $[C]_{\mathrm{Cl}}^{\mathrm{met}}$, and $[C]_{\mathrm{Cl}}^{\mathrm{sil}}$ are the metal-silicate partition coefficient of chlorine, the mass concentrations of chlorine in metal and silicate phase, respectively. a includes $\Delta S/R$, activity coefficients, and conversion factors from mole fraction to mass concentration. b and c correspond to $-\Delta H/R$ and $-\Delta V/R$, respectively. It is noted that equation (2.3) lacks compositional terms, such as the oxygen fugacity. This is because the speciation of chlorine in metallic and silicate phase has been poorly constrained. Therefore, compositional terms should be added to equation (2.3) if the metal-silicate partitioning of chlorine varies with the oxygen fugacity and chemical compositions of

metals and silicates. In the following sections, we experimentally investigate the effects of pressure and temperature on the metal-silicate partition coefficient of chlorine for a given composition using equation (2.3).

2.3. High pressure and temperature experiments

2.3.1. Starting materials

Chemical compositions of starting materials are listed in Table 2.1. Starting materials were prepared from a mixture of 70 wt% high-purity oxides (SiO_2, Al_2O_3, CaO, FeO, MgO), 23 wt% either iron (Fe) or sulfide (FeS), and 7 wt% $FeCl_2$ as a source of chlorine. The relative abundances of each component in the silicate portion were either CI- or EH-chondrites (Wasson and Kallemeyn, 1988), and the amount of FeO was close to be the present terrestrial mantle value (e.g., Wanke and Dreibus, 1988; McDonough and Sun, 1995). The range of oxygen fugacity (f_{O_2}) of these mixtures is approximately estimated to 1.5 ± 0.5 log units below iron-wüstite (IW) buffer (Frost et al., 2008). A pure sulfide was considered because sulfide is more stable than iron metal when a magma ocean becomes more oxidizing conditions (Wood and Halliday, 2005; Wood et al., 2006). In addition, sulfide generally affects the partition coefficients of elements between metallic liquid and silicate melts (e.g., Wade et al., 2012; Wood et al., 2014). The late segregation of sulfur into the core is also indicated by Mo and W (Wade et al., 2012) and the isotope ratio of Cu (Savage et al., 2015).

It is noted that chlorine abundance in our starting materials is much greater than that in chondrites. However, Henry's law may be acceptable up to wt% levels (Beattie, 1993), and therefore, high chlorine abundance used in this study would not strongly affect partition coefficient. All mixtures were grinded and homogenized under ethanol, and

dried at 383 K for at least 6 hours. Then, starting materials were stored in a desiccator to avoid water contamination.

Table 2.1. Chemical composition of starting materials (wt%).

	Fe metal + CI-like silicate	FeS metal + CI-like silicate	Fe metal + EH-like silicate	FeS metal + EH-like silicate
Silicate				
SiO_2	34.9		41.0	
Al_2O_3	2.5		1.8	
FeO	5.6		5.6	
CaO	2.0		1.4	
MgO	25.0		20.2	
Metal				
Fe	23.0	-	23.0	-
FeS	-	23.0	-	23.0
$FeCl_2$	7.0	7.0	7.0	7.0

2.3.2. Multi-anvil press experiments

High pressure and temperature experiments were carried out using multi-anvil presses: a 700 tonne wedge-type press (21mm cubic edge-length / 16 mm tungsten carbide anvil truncation edge-length) for 4 GPa at Institute for Solid State Physics, the University of Tokyo and a 3000 tonne Kawai-type press (11mm octahedral edge-length / 5 mm tungsten carbide anvil truncation edge-length) for 16-23 GPa at Geodynamics Research Center, Ehime University. The cell assemblies are shown in Figure 2.2. In each multi-anvil apparatus, pressures were estimated from pressure-load calibration curves based on the phase transition points of Bi, Tl and Ba for a 700 tonne wedge-type press, and ZnS, GaAs,

and GaP for a 3000 tonne Kawai-type press. Starting mixtures were encapsulated into either a graphite capsule or a single-crystal MgO capsule. We used these two types of capsules for the following reasons. First, metallic phase becomes saturated with carbon during experiments because carbon is siderophile. Moreover, previous studies have found that the carbon-saturated metallic liquid strongly influences the metal-silicate partitioning of some elements (e.g., Wood and Halliday, 2010). Thus, two types of capsules were used to investigate the effect of capsule materials on the metal-silicate partition behavior of chlorine.

Temperature was monitored using $W_{97}Re_3$- $W_{75}Re_{25}$ thermocouples located above the capsule at 4 GPa. For higher pressure experiments, because Re heater was frequently unstable using the W-Re thermocouples in our cell assembly, the power/temperature relation was used at 2473 K and 2673 K in which case temperature was estimated by extrapolating the power/temperature relation. The pressure effect on the thermocouple emf was not considered. The experiments were pressurized at room temperature in 1.5 hours for 4 GPa and 3 hours for 16-23 GPa. Samples were then heated to a run condition at 100 K/min. Run duration was varied to investigate an equilibrium attainment for low-temperature experiments. For high-temperature experiments (> 2123 K), run durations were 2~15 min in which cases time scale were estimated to be sufficient for chemical equilibration by previous reports (e.g., Thibault and Walter, 1995). Shorter durations were needed for experiments using a single-crystal MgO capsule due to a rapid dissolution of Mg into silicate melts. Experiments were quenched by turning off the power to heater.

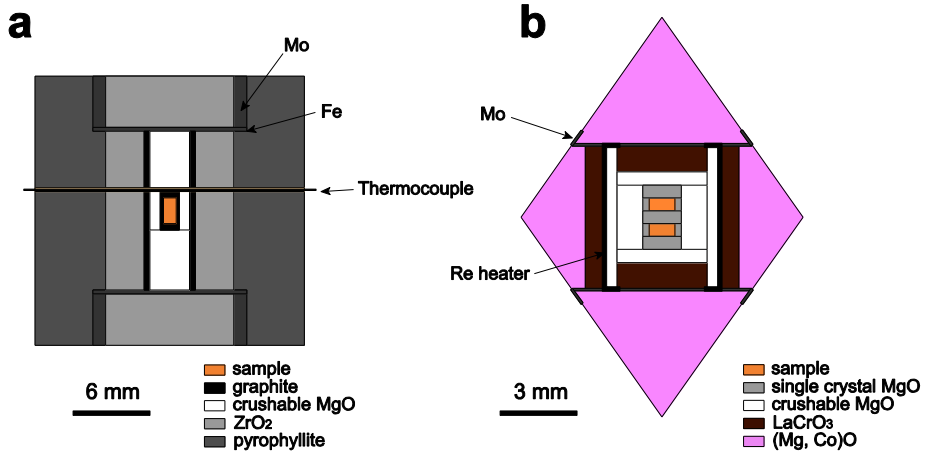

Figure 2.2. Cell assemblies for multi-anvil experiments used in this study. The left cubic cell (a) was used for a 700 tonne wedge-type press. The right octahedral cell (b) was used for a 3000 tonne Kawai-type press.

2.4. Analytical methods

2.4.1. Electron microprobe analysis

Recovered samples were mounted in epoxy and polished using SiC and diamond power under kerosene to avoid loss of chlorine in samples during preparations. The polished samples were then dried at room temperature in a vaccum chamber for 1 day. For EPMA analyses, the samples and standards were coated with a carbon film. The chemical composition of recovered samples were determined by a JEOL JXA-8900R electron microprobe analyzer (EPMA) at Atmospheric Ocean Research Institute, the University of Tokyo. Wavelength-dispersive spectrometry (WDS) analyses were conducted with an accelerating voltage of 15 kV, a beam current of 60 nA for major elements and 100 nA for chlorine in iron-rich metals. For silicate melts, a 20 μm defocused beam spot was applied to average quench textures. For metallic phase, a 10 μm defocused beam spot was applied. Because the distribution of chlorine in iron-rich metals was heterogeneous, an analytical uncertainty in one measurement is very large. Thus, analytical spots covered

almost entire area of the metallic phase to estimate the average concentration of chlorine in bulk metallic liquids. It is note that the near-interface between metal and silicate was not analyzed because precise analyses cannot be performed due to the presence of cracks and concaves. Peak counting times were 20s for Major elements and 60s for minor elements, respectively. Background counting times were a half of peak counting times. Pure iron (Fe), sulfide (FeS_2), and NIST glass standards (93a and K326) were used as standards for quantitative analyses using ZAF correction procedures. This analytical condition for WDS gives the detection limit of 20 ppm for chlorine. The detection limit was also confirmed using a pure-iron standard.

2.4.2. Secondary ion mass spectrometry analysis

In order to investigate the distribution of chlorine in metallic liquids, we performed mapping analyses both on iron-rich metallic liquids and sulfides using CAMECA NanoSIMS 50 ion microprobe at Atmospheric Ocean Research Institute, the University of Tokyo. For SIMS analyses, we re-polished the carbon-coated surface of the samples using diamond powders under kerosene. The re-polished samples were dried at about 50 ^{o}C in a vaccum chamber for 3 days. Then, the samples were coated with a gold film. A Cs^+ primary beam with a beam current of 50 pA, and an accelerating voltage of 16 kV was used. $^{37}Cl/^{56}Fe$ mapping images were acquired on a 100 × 100 μm^2 area at a resolution of 256 × 256 pixels by multi-collector mode with a dwell time of 40 ms/pixel. Prior to acquire mapping images, a pre-sputtering was performed for an hour to remove contamination on the sample surface.

Table 2.2. Experimental conditions.

Run No.	*P* / GPa	*T* / K	Run duration / min	Capsule	Starting composition
ISSP-1	4	1923	5	Graphite	Fe metal + CI-like silicate
ISSP-2	4	1923	10	Graphite	Fe metal + CI-like silicate
ISSP-3	4	1923	15	Graphite	Fe metal + CI-like silicate
ISSP-4	4	1923	30	Graphite	Fe metal + CI-like silicate
ISSP-5	4	1923	60	Graphite	Fe metal + CI-like silicate
ISSP-6A	4	1923	30	Graphite	Fe metal + EH-like silicate
ISSP-6B	4	1923	30	Graphite	FeS metal + EH-like silicate
ISSP-7A	4	2023	15	Graphite	Fe metal + CI-like silicate
ISSP-7B	4	2023	15	Graphite	FeS metal + CI-like silicate
ISSP-8A	4	2023	30	Graphite	Fe metal + EH-like silicate
ISSP-8B	4	2023	30	Graphite	FeS metal + EH-like silicate
ISSP-9A	4	2123	15	Graphite	Fe metal + CI-like silicate
ISSP-9B	4	2123	15	Graphite	FeS metal + CI-like silicate
ISSP-10A	4	2223	15	Graphite	Fe metal + EH-like silicate
ISSP-10B	4	2223	15	Graphite	FeS metal + EH-like silicate
ISSP-11A	4	2173	3	MgO	Fe metal + EH-like silicate
ISSP-11B	4	2173	3	MgO	FeS metal + EH-like silicate
GRC-1A	16	2473	2.5	MgO	Fe metal + EH-like silicate
GRC-1B	16	2473	2.5	MgO	FeS metal + EH-like silicate
GRC-2A	23	2673	2	MgO	Fe metal + EH-like silicate
GRC-2B	23	2673	2	MgO	FeS metal + EH-like silicate

2.5. Results

2.5.1. Quench textures and major element compositions

Figure 2.3 shows the back scattered image and the line profile of chlorine at the near metal-silicate boundary of the recovered sample. A spherical body of metals and no zonation of chlorine at the near metal-silicate boundary indicate completely molten iron and silicate, and chemical equilibrium attainment of chlorine partitioning. Here, it is noted that chlorine detected in run products by EPMA analyses is not contamination. This is because EPMA analyses did not detect chlorides combined with alkaline metals which were not included in our starting materials, such as sodium, potassium, and zinc. A finely-grained texture in silicate melts was observed for experiments using a graphite capsule, whereas a relatively coarsely-grained texture which is composed of quench crystals and glass, was observed for experiments using a single-crystal MgO capsule. Primary crystals, probably olivine and/or ferropericlase, were also observed for experiments using a single-crystal MgO capsule. No presence of bubbles was observed, suggesting that an exsolution of chlorine during quenching did not occurred.

Figure 2.4 shows the SIMS mapping of chlorine in iron-rich metal and sulfide. The large heterogeneous distribution of chlorine was observed. In particular, hot spots were seen for iron-rich metals. This result is consistent with large errors of chlorine abundances in an iron-rich metal shown in the previous study (Sharp and Draper, 2013). EPMA analyses and mapping images by SIMS analyses suggest that chlorine in metallic liquids may be present as immiscible phase.

Chemical compositions of recovered samples are shown in Table 2.3 and 2.4. EPMA analyses suggest that major elemental compositions of recovered samples were homogenous. A large difference in the amount of FeO was observed. For S-free

experiments using a graphite capsule, the amount of FeO in silicate melts increased relative to the value of starting materials. This might be as a result of the dissolution of Fe into silicate melts via decomposition of $FeCl_2$. In contrast, for some experiments using a single-crystal MgO capsule, FeO-poor silicate melts were observed, which is consistent with previous studies (e.g., Rose-Weston et al., 2009). This may be caused by a crystallization of ferropericlase which absorbs FeO. Systematically elevated MgO concentrations were also observed for a single-crystal MgO capsule due to the dissolution of Mg into silicate melts during experiments.

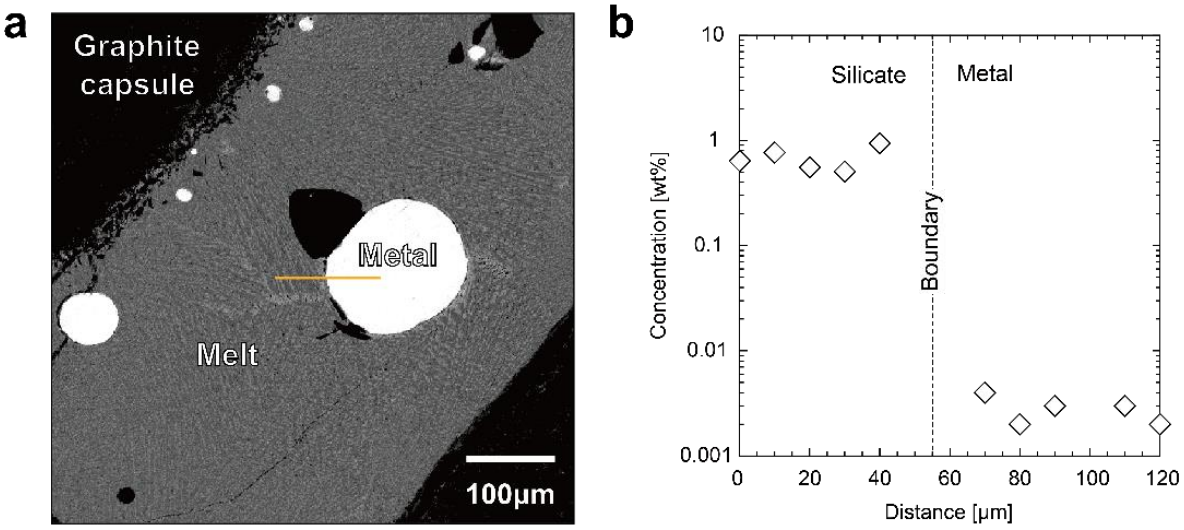

Figure 2.3. A back scattered electron image of typical quenching texture (ISSP-10A at 4 GPa and 2223 K). (a) A run product in a graphite capsule shows a finely-grained texture. A spherical body of metal indicates the complete molten in silicate melts. (b) The line profile of chlorine concentrations along the orange solid line shown in Figure 3a. A lack of data at the metal-silicate boundary is due to the presence of crack and surface roughness at which precise EPMA analyses cannot be performed. The line profile shows no obvious zonation at the near metal-silicate boundary, suggesting that chemical equilibrium was achieved.

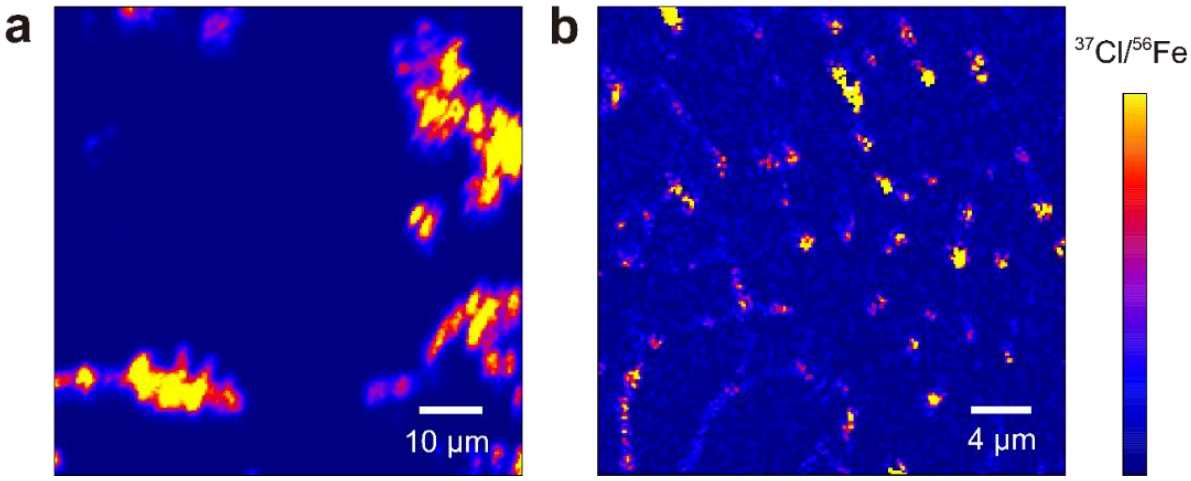

Figure 2.4. NanoSIMS mapping images of chlorine of typical quenching metallic liquids (a. ISSP-10A at 4 GPa and 2223 K, b. ISSP-10B at 4 GPa and 2223 K). (a) A 10 μm-scale hot spot was observed for iron-rich metals. The distribution of hot spots was large heterogeneity, but it shows no zonation. (b) The distribution of chlorine is heterogeneous in a μm scale, but homogeneous in a 10 μm-scale.

2.5.2. Oxygen fugacity

Oxygen fugacity is a key controlling factor on metal-silicate partitioning of elements. In the case of coexisting iron metal and iron oxide, oxygen fugacity (f_{O_2}) is controlled by iron-wüstite (IW) buffer. Thus, f_{O_2} during experiments was estimated from iron-wüstite (IW) buffer relation as follows:

$$\log f_{O_2}(\Delta IW) = 2\log\left(\frac{X_{FeO}^{sil}\gamma_{FeO}^{sil}}{X_{Fe}^{met}\gamma_{Fe}^{met}}\right) \quad (2.4)$$

where $f_{O_2}(\Delta IW)$, X_{FeO}^{sil}, X_{Fe}^{met}, γ_{FeO}^{sil}, and γ_{Fe}^{met} are the oxygen fugacity relative to IW-buffer, the mole fraction of FeO in silicate and Fe in metal, and the activity coefficient of FeO in silicate and Fe in metal, respectively. In this study, we assumed an ideal behavior for iron in metallic phase in which case the activity γ_{Fe}^{met} is 1. Although iron in liquid Fe-S alloys does not follow an ideal behavior, the difference of the oxygen fugacity

between an ideal model and a non-ideal model is within 0.5 log-units (Bouhifd et al., 2007). The value of $\gamma_{\mathrm{FeO}}^{\mathrm{sil}}$ was taken to be 1.7 proposed by Holzheid et al. (1997). The calculated values of f_{O_2} were within 1.5±1.0 log units below the IW buffer, which is the relevant values for the late core-mantle differentiation (e.g., Wade and Wood, 2005; Wood et al., 2006; Rubie et al., 2011; Cartier et al., 2014). In our experiments, no effect of the oxygen fugacity on the metal-silicate partitioning of chlorine was observed.

2.5.3. Analytical uncertainties

EPMA and SIMS mapping analyses show that the heterogeneous distributions of chlorine in both metallic and silicate phases. In particular, the scale of the heterogeneity of chlorine distributions in iron-rich metallic liquids is much larger than the size of EPMA analytical spots. In such cases, the standard deviation is not appropriate because the aim of this study is to determine the average value of bulk metallic liquids and silicate melts. To estimate analytical uncertainties on the average value, we used the standard error of the mean, which is the standard deviation divided by the square root of a number of analyses. As already proposed in previous studies (e.g., Walker et al., 1993; Thibault and Walter, 1995), this is better to represent an error of the average value on the elemental abundances of quenched heterogeneous textures.

The errors on the metal-silicate partition coefficient of chlorine were described by the following equation:

$$\Delta D_{\mathrm{Cl}}^{\mathrm{met/sil}} = D_{\mathrm{Cl}}^{\mathrm{met/sil}} \times \left(\frac{\Delta [C]_{\mathrm{Cl}}^{\mathrm{met}}}{[C]_{\mathrm{Cl}}^{\mathrm{met}}} + \frac{\Delta [C]_{\mathrm{Cl}}^{\mathrm{sil}}}{[C]_{\mathrm{Cl}}^{\mathrm{sil}}} \right) \quad (2.5)$$

where $D_{\mathrm{Cl}}^{\mathrm{met/sil}}$, $[C]_{\mathrm{Cl}}^{\mathrm{met}}$, $[C]_{\mathrm{Cl}}^{\mathrm{sil}}$, $\Delta[C]_{\mathrm{Cl}}^{\mathrm{met}}$, and $\Delta[C]_{\mathrm{Cl}}^{\mathrm{sil}}$ are the metal-silicate partition coefficient of chlorine, the concentration of chlorine in metallic liquids and silicate melts, the uncertainties on $[C]_{\mathrm{Cl}}^{\mathrm{met}}$ and $[C]_{\mathrm{Cl}}^{\mathrm{sil}}$, respectively.

Table 2.3. Chemical compositions of S-free recovered samples determined by EPMA-WDS (wt.%).

Run No.	ISSP-1	ISSP-2	ISSP-3	ISSP-4	ISSP-5	ISSP-6A	ISSP-7A
Silicate							
SiO_2	44.36 ± 0.79 [a]	44.95 ± 0.49	43.50 ± 0.22	40.82 ± 0.55	35.66 ± 0.09	45.19 ± 0.27	40.46 ± 0.19
Al_2O_3	3.61 ± 0.09	3.69 ± 0.12	2.51 ± 0.03	2.28 ± 0.10	2.83 ± 0.09	2.44 ± 0.01	1.98 ± 0.03
FeO	17.73 ± 0.25	17.08 ± 0.26	22.29 ± 0.25	23.65 ± 0.42	23.54 ± 0.08	23.56 ± 0.17	29.20 ± 0.20
CaO	1.09 ± 0.13	1.11 ± 0.10	0.61 ± 0.02	1.44 ± 0.16	1.81 ± 0.07	1.63 ± 0.06	0.70 ± 0.02
MgO	32.49 ± 0.44	33.27 ± 0.75	30.00 ± 0.14	26.93 ± 0.42	34.54 ± 0.32	23.57 ± 0.19	25.46 ± 0.13
Cl	0.99 ± 0.17	0.67 ± 0.10	0.84 ± 0.06	1.75 ± 0.22	1.12 ± 0.04	1.80 ± 0.08	1.71 ± 0.07
Total	100.26	100.76	99.75	96.87	99.50	98.18	99.50
N [b]	20	20	20	19	20	19	20
Metal							
Fe	92.62 ± 0.12 [c]	93.39 ± 0.07	95.13 ± 0.07	92.42 ± 0.17	92.02 ± 0.15	92.87 ± 0.11	92.69 ± 0.36
Cl / ppm	682 ± 80	75 ± 19	318 ± 9	94 ± 9	162 ± 102	32 ± 3	488 ± 101
Total	92.69 [c]	93.39	95.16	92.43	92.03	92.87	92.74
N	20	50	20	40	36	20	12
log fO_2 (ΔIW)	-1.30	-1.34	-1.87	-0.99	-1.05	-1.00	-0.83
NBO/T	2.57	2.56	2.70	2.77	3.68	2.30	2.90
$D_{Cl}^{met/sil}$	6.9 (± 2.0) × 10^{-2}	1.1 (± 0.8) × 10^{-2}	3.8 (± 0.4) × 10^{-2}	5.4 (± 1.2) × 10^{-3}	1.4 (± 1.0) × 10^{-3}	1.8 (± 0.2) × 10^{-3}	2.9 (± 0.7) × 10^{-2}

[a] Standard error of the mean.

[b] Number of analyses.

[c] The lack of mass may be largely due to solved carbon which is not analyzed.

Table 2.3 (*continued*). Chemical compositions of S-free recovered samples determined by EPMA-WDS (wt.%).

Run No.	ISSP-8A	ISSP-9A	ISSP-10A	ISSP-11A	GRC-1A	GRC-2A
Silicate						
SiO_2	45.62 ± 0.31	37.60 ± 0.09	40.98 ± 0.23	33.21 ± 0.72	36.81 ± 0.49	43.48 ± 0.48
Al_2O_3	1.61 ± 0.04	2.91 ± 0.09	1.71 ± 0.01	0.85 ± 0.35	1.63 ± 0.12	1.22 ± 0.04
FeO	25.01 ± 0.52	24.76 ± 0.09	28.49 ± 0.14	6.97 ± 0.55	11.00 ± 0.31	10.96 ± 0.32
CaO	0.82 ± 0.05	0.98 ± 0.03	0.67 ± 0.02	0.73 ± 0.10	0.47 ± 0.04	0.31 ± 0.02
MgO	25.82 ± 0.18	33.09 ± 0.34	23.94 ± 0.13	58.43 ± 0.55	47.93 ± 1.08	46.10 ± 0.32
Cl	1.12 ± 0.12	1.26 ± 0.04	1.38 ± 0.05	0.39 ± 0.05	0.42 ± 0.04	0.32 ± 0.02
Total	100.00	100.59	97.17	100.58	98.26	102.40
N	20	20	20	19	12	20
Metal						
Fe	93.34 ± 0.07	93.57 ± 0.09	93.75 ± 0.16	97.86 ± 0.19	94.13 ± 0.13	98.44 ± 0.15
Cl / ppm	243 ± 46	104 ± 43	2077 ± 337	437 ± 96	345 ± 125	429 ± 21
Total	93.36	93.58	93.96	97.90	94.16	98.48
N	20	40	27	20	19	40
log fO_2 (ΔIW)	-0.97	-1.83	-1.58	-2.23	-1.74	-1.79
NBO/T	2.50	3.39	2.76	5.48	4.16	3.47
$D_{\mathrm{Cl}}^{\mathrm{met/sil}}$	2.2 (± 0.7) × 10^{-2}	8.2 (± 3.7) × 10^{-3}	1.5 (± 0.3) × 10^{-1}	1.1 (± 0.4) × 10^{-1}	8.2 (± 3.8) × 10^{-2}	1.3 (± 0.8) × 10^{-1}

Table 2.4. Chemical compositions of S-bearing recovered samples determined by EPMA-WDS (wt.%).

Run No.	ISSP-6B	ISSP-7B	ISSP-8B	ISSP-9B	ISSP-10B	ISSP-11B	GRC-1B	GRC-2B
Silicate								
SiO_2	48.79 ± 0.62	48.10 ± 0.27	50.24 ± 0.24	34.20 ± 0.29	46.08 ± 0.71	30.26 ± 1.09	34.87 ± 0.87	42.25 ± 0.68
Al_2O_3	2.90 ± 0.05	2.56 ± 0.04	2.65 ± 0.05	2.89 ± 0.19	2.57 ± 0.06	0.86 ± 0.29	2.15 ± 0.17	1.63 ± 0.05
FeO	13.04 ± 0.58	12.05 ± 0.20	11.07 ± 0.17	10.14 ± 0.19	12.44 ± 0.50	4.26 ± 0.36	4.68 ± 0.18	3.28 ± 0.09
CaO	2.63 ± 0.20	1.78 ± 0.06	1.80 ± 0.08	2.54 ± 0.29	1.23 ± 0.14	0.84 ± 0.16	1.20 ± 0.07	0.93 ± 0.07
MgO	26.14 ± 0.32	27.04 ± 0.23	30.67 ± 0.30	47.99 ± 0.57	32.70 ± 0.43	62.27 ± 1.09	52.76 ± 0.91	50.78 ± 0.77
S	0.90 ± 0.33	0.44 ± 0.05	0.47 ± 0.06	0.42 ± 0.06	0.26 ± 0.05	0.79 ± 0.10	0.12 ± 0.02	0.30 ± 0.07
Cl	1.59 ± 0.14	1.92 ± 0.08	1.27 ± 0.06	0.42 ± 0.02	0.99 ± 0.09	0.31 ± 0.08	0.95 ± 0.07	0.65 ± 0.04
Total	96.00	93.89	98.16	98.6	96.27	99.59	96.74	99.83
N	17	20	20	20	20	9	20	20
Metal								
Fe	60.35 ± 0.24	60.17 ± 0.10	60.86 ± 0.05	62.58 ± 0.11	62.10 ± 0.06	60.73 ± 0.19	61.39 ± 0.15	62.67 ± 0.14
S	35.64 ± 0.18	35.58 ± 0.18	36.35 ± 0.10	33.94 ± 0.11	35.96 ± 0.06	34.39 ± 0.15	35.55 ± 0.03	35.65 ± 0.11
Cl / ppm	4152 ± 342	1734 ± 163	2603	1264 ± 103	1906 ± 107	688 ± 124	565 ± 38	1416 ± 102
Total	96.40	95.92	97.47	96.65	98.24	95.20	97.01	98.46
N	20	19	20	20	24	20	20	20
log fO_2 (ΔIW)	-0.86	-0.97	-1.08	-0.43	-0.22	-2.20	-1.91	-2.25
NBO/T	1.96	2.00	2.08	4.33	2.41	6.23	4.44	3.57
$D_{Cl}^{met/sil}$	2.6 (± 0.5) × 10^{-1}	9.0 (± 1.2) × 10^{-2}	2.1 (± 0.2) × 10^{-1}	3.0 (± 0.4) × 10^{-1}	1.9 (± 0.3) × 10^{-1}	2.2 (± 0.9) × 10^{-1}	6.0 (± 0.8) × 10^{-2}	2.2 (± 0.3) × 10^{-1}

2.5.4. Equilibrium attainment of $D_{\mathrm{Cl}}^{\mathrm{met/sil}}$

To estimate a time scale for partition-equilibrium attainment, different duration-time experiments were conducted at 4GPa and 1923 K. Figure 2.5 shows the metal-silicate partition coefficient of chlorine as a function of run durations. At 1923 K, a metal-silicate partition equilibrium of chlorine was appear to be achieved at 30 min. An equilibrium attainment of metal-silicate partitioning of chlorine was also indicated by no zonation at the metal-silicate boundary. Although run durations were shorter than 30 min (i.e., 3~15 min) at higher temperatures above 2123K, these run durations are thought to be sufficient for chemical equilibrium as mentioned above and also indicated by compositional homogeneities in quench textures of recovered samples.

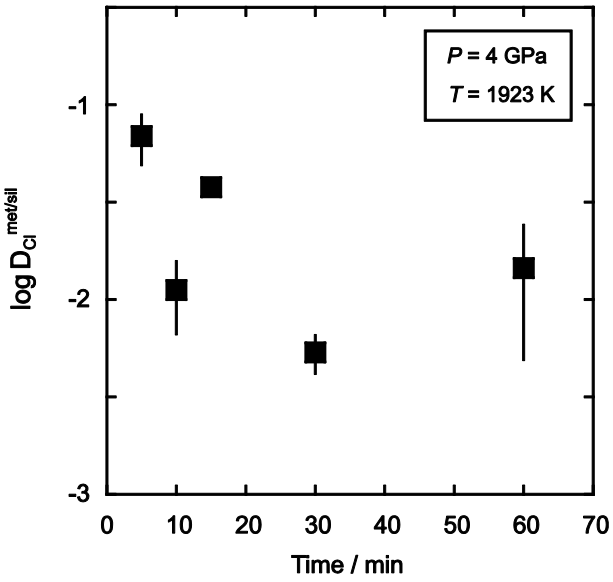

Figure 2.5. Time series for metal-silicate partition coefficients of chlorine at 4GPa and 1923 K. Partitioning equilibration is achieved after 30 min, though the variation is still large due to the large uncertainties of chlorine abundance in metallic liquids. The equilibrium attainment was also confirmed by observation of quenching textures (see text).

2.5.5. The effect of pressure and temperature on $D_{\mathrm{Cl}}^{\mathrm{met/sil}}$

Figure 2.6 shows the metal-silicate partitioning of chlorine as a function of temperature at 4 GPa. In our experimental conditions, all of the metal-silicate partition coefficients of chlorine are below the unity, suggesting that chlorine is a lithophile element. For a S-free system, chlorine becomes slightly siderophile with increasing temperature. For a S-bearing system, the metal-silicate partition coefficient of chlorine is generally higher than that for a S-free system especially at low-temperature experiments. In contrast to a S-free system, no effect of temperature on the sulfide-silicate partitioning of chlorine was observed. This result is consistent with the previous study although the metal-silicate partition coefficient in our study are slightly higher than previous one (Mungall and Brenan, 2003)

Figure 2.7 shows the metal-silicate partitioning of chlorine as a function of pressure. For a S-free system, pressure decreases the metal-silicate partitioning of chlorine, suggesting that the incorporation of chlorine into a metal droplet at the deep magma ocean would be limited even though high temperature conditions likely elevate the siderophile behavior of chlorine. In contrast, for a S-bearing system, no effect of pressure was observed as shown in a temperature dependency.

2.5.6. The effect of metal and silicate compositions on $D_{\mathrm{Cl}}^{\mathrm{met/sil}}$

Capsule materials affects both on metallic and silicate compositions. As mentioned above the section 2.3.2., a graphite capsule changes the chemical composition of metallic liquids during experiments because carbon dissolves in metallic phase up to several wt.% (e.g., Wood, 1993; Dasgupta and Walker, 2008). In this study, the metal-silicate partition coefficient of chlorine for a single-crystal MgO capsule was within the range for a

graphite capsule in both cases of iron and sulfide at 4 GPa (see Figure 2.6). In addition, the concentrations of chlorine in metallic liquids for the case of a single-crystal MgO capsule were also within the range of experiments. Thus, our data that chlorine is a moderately to highly lithophile element, would be valid.

In contrast to a graphite capsule, a MgO capsule changes the chemical compositions of silicate phase. Previous studies have reported that chlorine becomes more soluble as hydrous alkaline silicate melts become more depolymerized (high number of non-bridging oxygen/tetrahedral cation, NBO/T) (e.g., Signorelli and Carroll, 2002). In our experiments, the abundance of chlorine in silicate melts broadly decreases with increasing NBO/T, which is the opposed results to previous studies. In contrast, chlorine in silicate melts was positively correlated with the abundance of Fe in silicate melts in our experiments. Given that chlorine in Fe-rich silicate melts preferentially bonds to Fe^{2+} (Filiberto and Treiman 2009; Filiberto et al., 2014), the differences of chlorine solubility in silicate melts between the present study and previous studies are probably due to the compositional differences (i.e., FeO abundances). Although the abundance of chlorine in silicate melts varies with NBO/T and Fe^{2+} contents, no obvious effect of silicate compositions on $D_{\mathrm{Cl}}^{\mathrm{met/sil}}$ was observed. Thus, the compositional changes of a magma ocean would not have influenced chlorine partitioning between core and mantle.

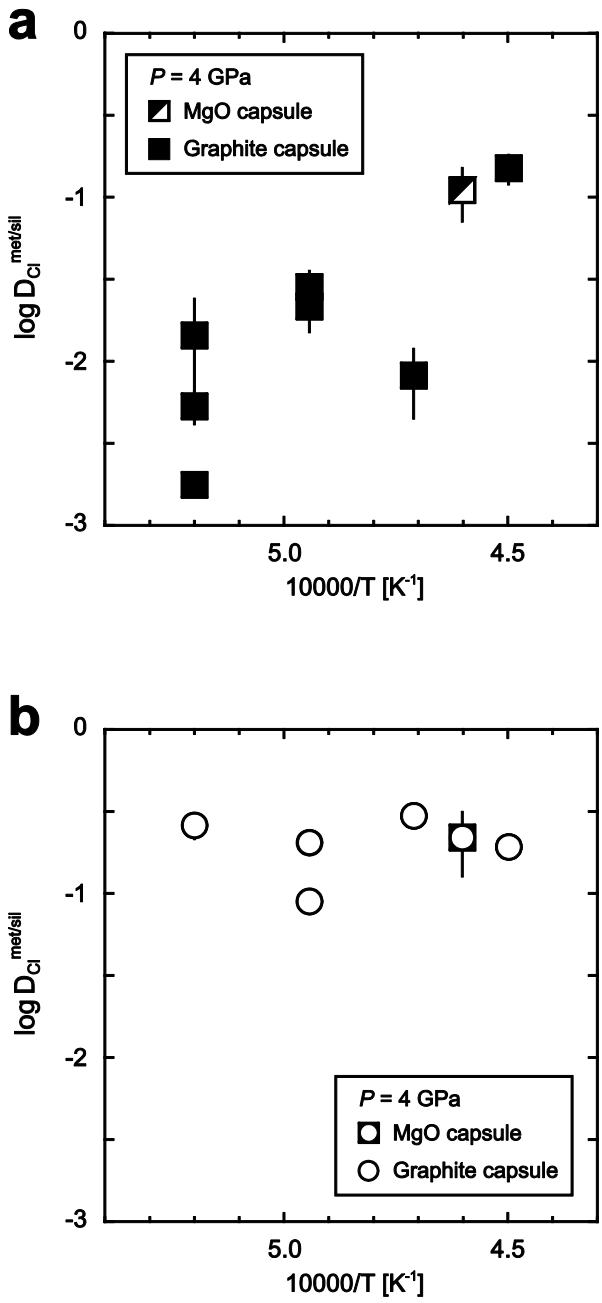

Figure 2.6. Metal-silicate partitioning coefficient of chlorine as a function of temperature. (a) Iron-silicate partitioning of chlorine depends on temperature. Chlorine becomes moderately siderophile with increasing temperature. (b) Sulfide-silicate partitioning of chlorine has no temperature dependency. As temperature increases, the difference of metal-silicate partition coefficients between iron and sulfide becomes small, and possibly the values reverse at higher temperature.

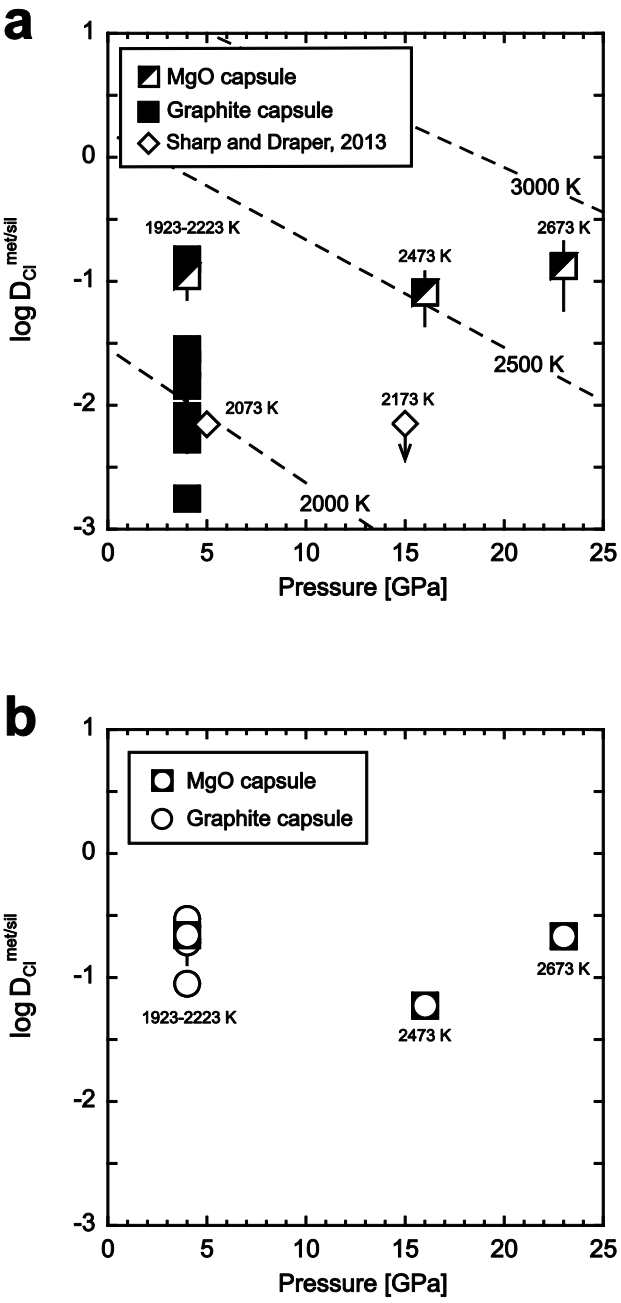

Figure 2.7. Metal-silicate partitioning coefficient of chlorine as a function of pressure. (a) The dashed lines indicate calculated values of metal-silicate partitioning coefficient using equation (6). Iron-silicate partitioning of chlorine decreases as pressure increases. (b) Sulfide-silicate partitioning of chlorine has also no pressure dependency.

3. Chlorine partitioning between silicate melts and minerals at the transition zone and lower mantle conditions.

3.1. Introduction

In the Chapter 2, we have shown that chlorine is highly lithophile elements at the range of *P-T* conditions investigated in the study. If terrestrial missing chlorine may not be in the Earth's core, there are two potential reservoirs for Earth's chlorine: the deep mantle and the primordial hydrosphere that has been lost to space. The deep reservoir for chlorine is important for estimating volatile budget of the bulk silicate Earth, whereas the geochemical evidence for an oceanic loss episode is a key for elucidating the origin of terrestrial hydrosphere. In the following, we consider the retention of chlorine in the deep mantle.

Given the modest compatible behavior of water and fluorine in deep mantle minerals, such as $(Mg,Fe)_2SiO_4$ wadsleyite, $(Mg,Fe)SiO_3$ bridgmanite and (Mg,Fe)O ferropericlase (e.g., Inoue et al., 1995; Murakami et al., 2002; Litasov et al., 2003; Bolfan-Casanova et al., 2003; Inoue et al., 2010; Litasov, 2012; Roberge et al., 2015), chlorine might also have been trapped in deep mantle minerals during magma ocean solidification. This is because the ionic radius of chlorine is relatively similar to that of OH and F. In addtion, water-enriched ringwoodite has been found in the diamond inclusions (Pearson et al., 2014), supporting the presence of water-rich reservoir in the deep mantle. Thus, given the similarity of chemical properties among OH, F^- and Cl, as a part of terrestrial chlorine might have been stored in the deep mantle. If so, terrestrial missing chlorine may have

been caused either by the incorporation into the deep mantle minerals during magma ocean solidification or the transport from the surface to deep mantle via subsequent tectonic activity. However, the transport of chlorine into the deep mantle via subduction is unlikely because the silicate mineral-melt and mineral-fluid partition coefficients of chlorine at the upper mantle conditions are generally quite low (e.g., Dalou et al., 2012; Fabbrizio et al., 2013a; 2013b). Moreover, the flux ratio of chlorine between subduction and outgassing at the subduction zone is approximately the unity (e.g., Straub and Layne, 2003), suggesting that terrestrial chlorine may not have been transported into the deep mantle due to the subduction barrier. It is therefore more likely that terrestrial chlorine was retained in the deep Earth's interior during magma ocean solidification. However, the deep mantle has not been considered previously as a potential reservoir for explaining terrestrial missing chlorine. In this study, we experimentally investigate chlorine partitioning between silicate melts and minerals at deep mantle conditions.

3.2. High pressure and temperature experiments

3.2.1. Starting materials

Starting materials were prepared from a high-purity oxide mixture of SiO_2, Al_2O_3, CaO, MgO, FeO, and $FeCl_2$ (see Table 3.1). The relative abundance of oxides with the exception of Al_2O_3 was chosen to be pyrolytic composition estimated from McDonough and Sun (1995). 2 wt% $FeCl_2$ was added to pyrolitic silicate mixtures as the source of chlorine. The Al_2O_3 content in starting materials is depleted relative to pyrolitic composition to crystallize bridgmanite instead of majorite. All mixtures were grinded and homogenized under ethanol and dried at 383 K for 12 hours. Dried mixtures were then stored in a desiccator to minimize contacting air.

Table 3.1. Chemical composition of starting materials (wt%).

	Al-depleted pyrolite
SiO_2	45.6
Al_2O_3	1.9
FeO	8.2
CaO	3.6
MgO	38.5
$FeCl_2$	2.2

3.2.2. Multi-anvil press experiments

Experiments were carried out at 18 GPa and 23 GPa using a 3000 tonne Kawai-type multi-anvil apparatus at Geodynamics Research Center, Ehime University. We used a 11/5 cell assembly (11 mm octahedral edge-length/5 mm tungsten carbide anvil truncation edge-length). Pressures were estimated from the pressure-load calibration curve based on the transition points of ZnS, GaAs, and GaP. Temperatures were estimated from the temperature-power calibration curve using $W_{97}Re_3$-$W_{75}Re_{25}$ thermocouples. For temperature calibration, no pressure effect on thermocouple emf was assumed. In this study, we did not monitor the temperature using thermocouples because Re heaters were often unstable when thermocouples inserted in heaters in our cell assembly.

Starting materials were encapsulated into unsealed rhenium-foil capsules surrounded by a MgO sleeve. Experiments were pressurized at room temperature in 3 hours. Then, samples were heated to a run temperature condition at 100 K/min and held for 20-30 min. Experiments were quenched by turning off the power to the heater.

3.3. Analytical methods

3.3.1. EPMA analysis for major elemental compositions

Recovered run products were amounted in epoxy and polished using SiC and 1, 3 μm diamond powders under kerosene to avoid loss of chlorine during sample preparations. The analyses on major elemental compositions of run products were conducted using a JEOL JXA-8900R electron microprobe analyzer (EPMA) with wavelength-dispersive spectroscopy (WDS) at Atmospheric and Ocean Research Institute, The University of Tokyo. Analytical conditions were an accelerating voltage of 15 kV and a beam current of 60 nA. A 20 μm defocused beam spot was used for analyze quenched silicate melts, whereas a 5-10 μm beam spot was used for crystals depending on the size. Peak-counting times were 20 s for major elements and 60 s for minor elements, respectively. Counting times for background were a half time of peak counting. NIST-93a and NIST-K326 glasses were used as standards. In order to identify mineral phases in quenched run products, micro-focused X-ray diffractmetry was also used (see Appendix 2 and 3).

3.3.2. SIMS analysis for chlorine in the mineral phase

Chlorine abundance in minerals was analyzed by a CAMECA NanoSIMS 50 ion microprobe at Atmosphere and Ocean Research Institute, The University of Tokyo. For secondary ion mass spectrometry (SIMS) analysis, samples were re-polished to remove carbon-coating surface. Then, the polished surface of the samples was coated with high-purity gold.

A 1 nA primary ion beam of Cs^+ with an accelerating voltage of 16 kV was used. For each analytical step, a pre-sputtering on a 20×20 μm area was conducted for 4 minutes before analysis to remove contamination on the sample surface, and then a primary beam

was focused on a 5×5 μm area for 200 seconds. The isotope ratios $^{35}Cl/^{30}Si$ and $^{35}Cl/^{56}Fe$ were measured for silicate minerals and ferropericlase, respectively. NIST-93a glass standard was used to determine chlorine abundances. The detection limit of this analytical method was confirmed using chlorine-free glass standard.

3.4. Results

Experimental conditions and chemical compositions of quenched run products are listed in Table 3.2. The back-scattered electron microprobe image and X-ray maps of the recovered run product at 23 GPa are shown in Figure 3.1. Quenched silicate melts in run products show that a finely-grained texture composed of quenched crystals and glass. Chemical compositions of quenched silicate melts were heterogeneous at a μm-scale, whereas homogeneous at a larger scale. The compositional heterogeneity in a micro-scale was probably dependent on a cooling rate during quenching. In such cases, the standard error of the mean is better to express analytical uncertainties in the average bulk compositions as proposed by the previous study (Thibault and Walter, 1995).

For the experiment at 18 GPa and 2273 K, the coexistence of silicate melts and wadsleyite was observed. For the experiment at 23 GPa and 2473 K, the coexistence of silicate melts, bridgmanite, and ferropericlase was obsereved. Each mineral phase was identified by elemental compositions and X-ray diffraction patterns. Compositional zonation at crystal-melt boundary was not observed. In addition, an approximately constant $^{35}Cl/^{30}Si$ ratio of mineral phases during SIMS analyses also indicates no vertical zonation of chlorine, suggesting that chlorine partitioning between silicate melts and minerals achieved to be equilibrium.

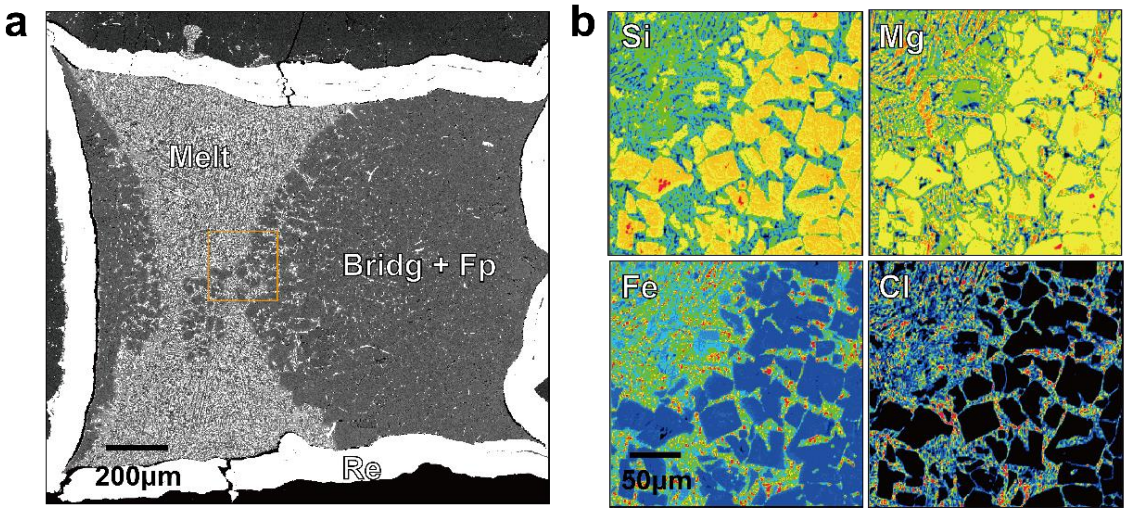

Figure 3.1. Back-scattered electron microprobe image and X-ray maps. **a**, Abbreviations for minerals used are: Bridg, Bridgmanite; Fp, Ferropericlase. **b**, Elemental distribution maps in a closer view of Figure 1a.

3.4.1. The mineral-melt partition coefficients of chlorine

As shown in the X-ray map of chlorine distribution (Figure 3.1b), chlorine is mainly partitioned into silicate melts at deep mantle conditions. The abundance of chlorine in wadsleyite, bridgmanite, and ferropericlase was much lower than that in silicate melts. Table 3.3 summarizes the mineral-melt partition coefficients of chlorine. The mineral-melt partition coefficients of chlorine at the transition zone and lower mantle conditions is very close to the values at upper mantle conditions reported in previous studies (e.g., Dalou et al., 2012). These results indicate that the solid part of Earth's mantle would not have retained chlorine during planetary differentiation. Thus, the primordial Earth's surface (i.e., primitive crust and/or hydrosphere) would have been a main reservoir of chlorine if the Earth's core was not missing chlorine reservoir.

Table 3.2. Chemical compositions of run products.

P / GPa	18			23	
T / K	2273			2473	
Run time / min	30			20	
Phase [a]	Melts	Wd	Melts	Bridg	Fp
EPMA					
SiO_2	46.1 ± 0.51 [b]	39.8 ± 0.09	38.9 ± 0.31	52.2 ± 0.31	0.06 ± 0.01
Al_2O_3	2.63 ± 0.13	0.35 ± 0.04	1.57 ± 0.04	2.32 ± 0.05	0.53 ± 0.01
FeO	7.69 ± 0.18	6.63 ± 0.08	11.7 ± 0.16	3.99 ± 0.07	13.2 ± 0.38
CaO	5.24 ± 0.18	0.06 ± 0.02	3.52 ± 0.14	0.65 ± 0.03	0.02 ± 0.00
MgO	33.3 ± 0.38	56.1 ± 0.08	37.6 ± 0.35	39.7 ± 0.30	86.6 ± 0.43
Cl	0.40 ± 0.03	-	0.97 ± 0.10	-	-
N [c]	18	19	20	31	9
SIMS					
Cl / ppm	-	3.4 ± 0.3	-	82.1 ± 7.5	35.9 ± 7.8
N	-	7	-	4	4
Total	95.3	103.0	94.3	98.8	100.4

[a] Abbreviation for minerals used are: Wd, wadsleyite; Bridg, bridgmanite; Fp, ferropericlase.

[b] Analytical uncertainties are expressed 1 standard error of the mean.

[c] Number of analyses

Table 3.3. Mineral-melt partition coefficients of chlorine.

	Values	References
$D^{\text{Olivine/melt}}$	1.2×10^{-3}	Dalou et al. [2012]
$D^{\text{Clinopyroxene/melt}}$	$1.7 \times 10^{-3} \sim 2.1 \times 10^{-2}$	Dalou et al. [2012]
$D^{\text{Orthopyroxene/melt}}$	$1.7 \times 10^{-3} \sim 2.8 \times 10^{-2}$	Dalou et al. [2012]
$D^{\text{Plagioclase/melt}}$	1.4×10^{-3}	Dalou et al. [2012]
$D^{\text{Wadsleyite/melt}}$	8.4×10^{-4}	This study
$D^{\text{Bridgmanite/melt}}$	8.5×10^{-3}	This study
$D^{\text{Ferropericlase/melt}}$	3.7×10^{-3}	This study

4. Implications for the origin of terrestrial missing chlorine

In this section, we discuss implications of experimental results for the origin of terrestrial missing chlorine. First, we discuss the core-mantle partitioning of chlorine during the differentiation of the Earth. Then, we discuss the distribution of chlorine during magma ocean solidification and the origin of terrestrial missing chlorine.

4.1. Core-mantle partitioning of chlorine during the formation of the Earth

For the metal-silicate partitioning of chlorine, the parameter coefficients of equation (2.3) for a S-free system were determined by multiple regression, yielding the following equation:

$$\log D_{Cl}^{\mathrm{met/sil}} = 7.11 - \frac{17{,}430}{T} - 175\frac{P}{T} \qquad (4.1)$$

where temperature term *T* and pressure term *P* are in K and GPa, respectively. Using this equation, we estimated the metal-silicate partition coefficient of chlorine at the relevant *P*-*T* conditions of core-mantle separation inferred from the abundance patterns of siderophile elements in the mantle (e.g., Wade and Wood, 2005). The predicted metal-silicate partition coefficient of chlorine at the mean *P*-*T* condition at the base of magma ocean estimated by Wade and Wood (2005) is estimated to be approximately 0.09. The calculated value is approximately two orders of magnitude lower than the required value estimated by previous studies (McDonough, 2003; Sharp and Draper, 2013). Thus, the incorporation of chlorine into the Earth's core is unlikely to be the origin of terrestrial missing chlorine. Although a single core stage model may not appropriate for the estimate of the core-mantle partition of elements, a continues accretion model cannot also explain terrestrial missing chlorine by core segregation as discussed in the following. For a

continues accreting model, the partitioning equilibration of elements between metallic liquids and silicate melts occurs at the base of a magma ocean where the metal pond layer locates above the solidus mantle. Therefore, the metal-silicate partition coefficient of elements at the liquidus *P-T* conditions of mantle would be required. Using the metal-silicate equilibration temperatures based both on the experimental results and a thermodynamic model (Rubie et al., 2015 and references therein), the values of $\log D_{\mathrm{Cl}}^{\mathrm{met/sil}}$ at the *P-T* conditions of the base of a magma ocean for a given accretion mass are much lower than the unity (see Figure 4.2), suggesting that almost all of chlorine would be partitioned to the mantle at the base of a magma ocean. This result strongly indicates that Earth's core may not be a missing chlorine reservoir. It is noted that these estimated values include a large uncertainty due to the large extrapolation of experimental data. However, given the low-equilibration efficiency between proto-Earth's magma oceans and the cores of large differentiated impactors, which is supported by the Hf-W isotope data (Halliday, 2004; Nimmo and Agnor, 2006; Nimmo et al., 2010; Rudge et al., 2010), a fluid dynamic study (Dahl and Stevenson, 2010), and multi-stage core-mantle differentiation models (Rubie et al., 2011; Rubie et al., 2015), the late incorporation of chlorine into Earth's core may be limited because chlorine must be partitioned planetary mantles during early accretion stage as shown in our experiments.

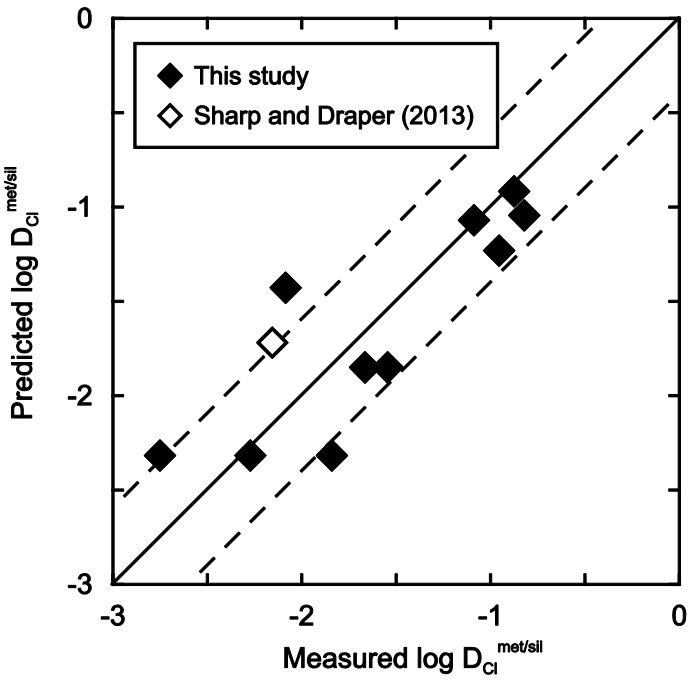

Figure 4.1. Comparison of the iron-silicate partition coefficient between experimentally determined values and predicted values using equation (4.1). The solid line indicates the 1 :1 correspondence. The dashed lines indicate the standard error.

Table 4.1. Experimental constraints on parameters for the $D_{\mathrm{Cl}}^{\mathrm{iron/sil}}$ parameterization.

	Parameters [a]	Standard error
a	7.11	2.64
b	-17430	5010
c	-175	104

[a] Parameters were determined by multiple regression using equation (2.3). The determination coefficient R^2 = 0.69

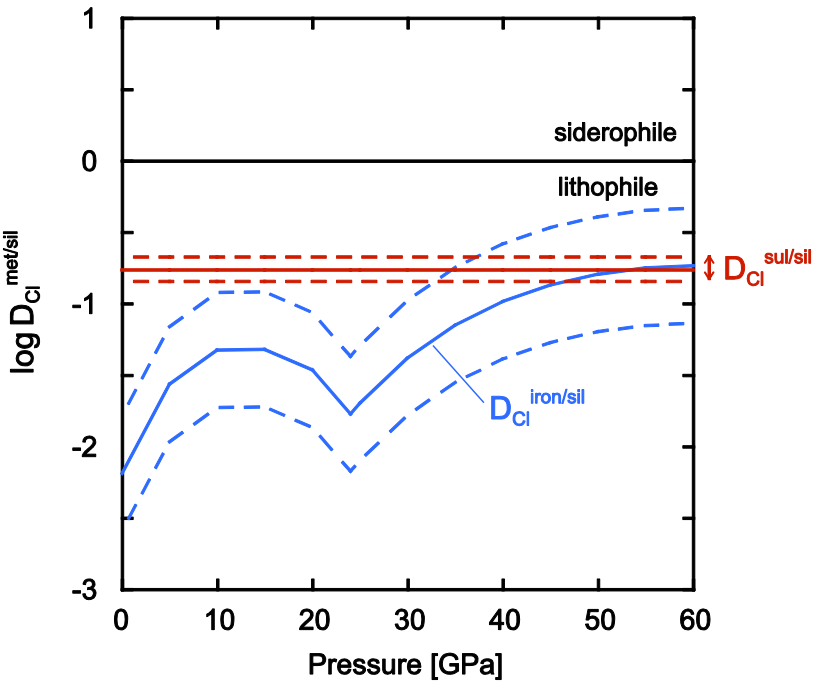

Figure 4.2. The metal-silicate partition coefficient of chlorine along the peridotite melting curve. The metal-silicate equilibration temperature was taken from Rubie et al. (2015). The solid curve indicates the iron-silicate partition coefficient of chlorine. The solid line indicates the average sulfide-silicate partition coefficient of chlorine in our experimental results, and the dashed lines indicate 1σ of the mean. This figure shows that chlorine should be partitioned to mantle during core-mantle differentiation.

4.2. Comparison with other volatile elements

In the above discussion, we have concluded that Earth's core is unlikely to be the reservoir of terrestrial missing chlorine. Moreover, the silicate mineral-melt partition experiments have shown that chlorine is highly incompatible with minerals. Our results have strongly indicated that the deep Earth's interior including core would not have stored chlorine during the main accretion phase. Thus, the primordial chlorine-rich reservoir of the Earth would have been lost to space. Given that the isotopic ratios of chlorine would be fractionated during the degassing of a magma ocean for lunar size proto-planets (Boyce

et al., 2015), terrestrial chlorine may not have been lost to space during early accretion stages because the isotopic compositions of terrestrial chlorine are within the values of chondrites (Sharp et al., 2007). If this is the case, chlorine-rich reservoir may have been lost by a collisional erosion during the late accretion stage, more specifically, a mantle-stipping impact (e.g., O'Neill and Palme, 2008; Campbell and O'Neill, 2012; Boujibar et al., 2015; Bonsor et al., 2015) and a loss of primordial oceans (e.g., Sharp and Draper, 2013; Tucker and Mukhopadhyay, 2014). In order to further constrain the origin of terrestrial missing chlorine, we discuss the abundance pattern of chlorine and other incompatible lithophile and volatile elements.

4.2.1. Cl/K and Cl/Zn ratios

Figure 4.3 shows the comparison of Cl/K and Cl/Zn ratios between the bulk silicate Earth and chondrites. As mentioned in the introduction, the Cl/K and Cl/K ratios of the Earth is lower than any types of chondrites, suggesting that the mantle-stipping erosion cannot explain the present Cl/K and Cl/Zn ratios. In order to fractionate the Cl/K and Cl/Zn ratios, a selective loss of chlorine is required.

Based on the oxygen isotopic composition and the iron content, the building blocks of the Earth may be the mixture of 4% CI-, 5% CV-, 21% H-, and 70% EH-chondrites. If this is the case, the Cl/K and Cl/Zn ratios of the predicted primitive Earth are approximately an order of magnitude lower than the present values: $(Cl/K)_{BSE}/(Cl/K)_{predicted}=0.10$ and $(Cl/Zn)_{BSE}/(Cl/Zn)_{predicted}=0.12$. This inference indicates that terrestrial chlorine may have been lost nearly 90 wt.% of its initial content during the accretion phase. Given such depletion of terrestrial chlorine relative to incompatible lithophile and moderately volatile elements, the most simple explanation

for the origin of terrestrial missing chlorine is a loss of primordial chlorine-rich hydrosphere as originally proposed by Sharp and Draper (2013). Chlorine at planetary surface would have partitioned into hydrosphere because the fluid-melt partition coefficient of chlorine is above the unity (e.g., Signorelli and Carroll, 2000; Métrich et al., 2001). Thus, the current Cl/K and Cl/Zn ratios of the Earth are consistent with the scenario of an extensive loss of primordial hydrosphere. During the presence of a magma ocean, chlorine would have been lost accompanied by the escape of a steam atmosphere. After the condensation of water, chlorine would have dissolved in a primitive ocean. Thus, an oceanic erosion would be required. Given the range of the fluid-melt partition coefficients of chlorine, the replacement of the primordial Earth's hydrosphere may have taken place at least one time. More specifically, the relation between the number n of replacement of the hydrosphere to account for the observed chlorine depletion for Earth depends on effective partition coefficient $D_{\mathrm{atm/mantle}}$ between atmosphere and mantle. Nevertheless, this dependence is rather weak; n depends on logarithm of $1+D_{\mathrm{atm/mantle}}$. The specific dependence can be given in a simple analytical form when a simple hydrosphere replacement scenario is assumed. The proportion of chlorine in the present Earth relative to the building blocks can be approximated by the following equation:

$$\frac{[C]^{\mathrm{Cl}}_{\mathrm{initial}}}{[C]^{\mathrm{Cl}}_{\mathrm{present}}} = \left(\frac{1}{1 + D^{\mathrm{Cl}}_{\mathrm{atm/mantle}}}\right)^{n} \tag{4.2}$$

Here, $[C]^{\mathrm{Cl}}_{\mathrm{initial}}$ and $[C]^{\mathrm{Cl}}_{\mathrm{present}}$ are the concentration of chlorine in the bulk silicate Earth at the initial and the present, respectively. $D^{\mathrm{Cl}}_{\mathrm{atm/mantle}}$ is the proportion of chlorine in the atmosphere relative to the mantle. n is the replacement frequency of the hydrosphere.

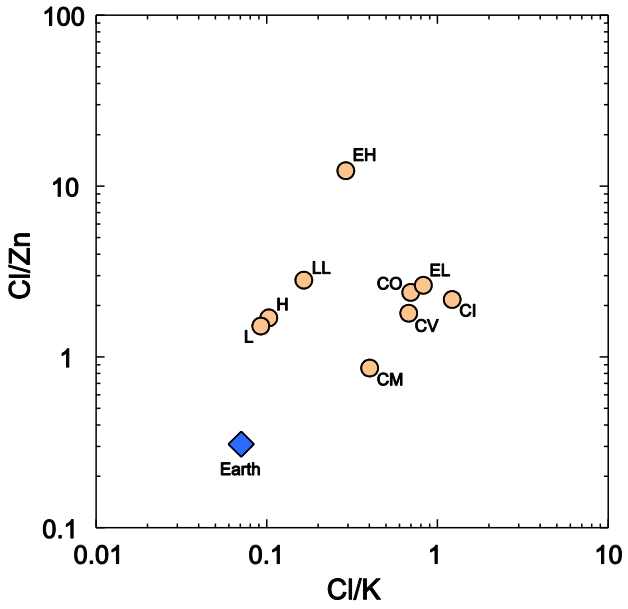

Figure 4.3. The Cl/Zn and Cl/K ratios of the Earth and chondrites. Data were taken from Wasson and Kallemeyn (1988) and McDonough and Sun (1995).

4.2.2. H_2O/Cl ratio

Because the mineral-melt partition coefficients of water is generally higher than that of chlorine (Hauri et al., 2006), residual silicate melts at the planetary surface may have had lower H_2O/Cl ratios compared to the deep mantle during magma ocean solidification. If this is the case, the H_2O/Cl ratio of a steam atmosphere over such a chlorine-rich magma ocean may also have been lower values relative to the bulk value. Thus, an extensive loss of terrestrial hydrosphere could have elevated the H_2O/Cl ratio of the residual bulk silicate Earth. In other words, the H_2O/Cl ratio of the Earth may be higher than the chondritic values.

Figure 4.4 shows variations of the H_2O/Cl ratio and water contents between the Earth and chondrites. Although the H_2O/Cl ratio of the Earth is similar to CI-chondrites (e.g.,

Marty, 2012), the mixture of chondritic components cannot explain both on the water content and the H_2O/Cl ratio of the Earth. Because the H_2O/Cl ratio of ordinary and enstatite chondrites is generally much lower than that of the Earth, the H_2O/Cl ratio of the primitive Earth may also have been lower than present one. More specifically, assuming that all of water of the Earth was received from chondritic materials as mentioned in the above section 4.2.1., the predicted H_2O/Cl ratio of the Earth is approximately an order of magnitude lower than the present value. The difference in H_2O/Cl ratios between the present Earth and the chondritic Earth might be explained by a loss of chlorine-rich primordial hydrosphere.

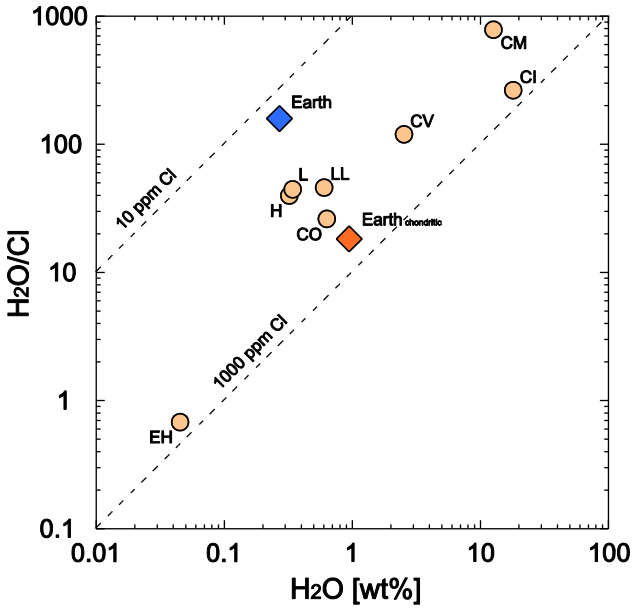

Figure 4.4. Comparison of the H_2O/Cl ratios and water contents among Earth and chondrites. Data for the Earth and chondrites were taken from Wasson and Kallemeyn (1988), McDonough and Sun (1995), Javoy (1998), and Schaefer and Fegley (2007). The value for the chondritic Earth was estimated from the model of Lodders (2000).

5. Summary

In this thesis, we have experimentally investigated chlorine partitioning between metallic liquids, silicate melts, and minerals in a magma ocean to assess the possibilities of the incorporation of chlorine into deep Earth's interior during the formation of the Earth. The results are as follows:

1. The iron-silicate partition coefficient of chlorine increases with increasing temperature and decreases with increasing pressure. In contrast, the sulfide-silicate partition coefficient of chlorine is not dependent both on pressure and temperature.
2. The predicted metal-silicate partition coefficient of chlorine at the mean *P*-*T* condition of core-mantle separation inferred from the abundance patterns of siderophile elements in the mantle is much lower than the required value for explaining terrestrial missing chlorine.
3. The silicate mineral-melt partition coefficients at the transition zone and lower mantle conditions were also much lower than the required value for explaining terrestrial missing chlorine. The incompatibilities of chlorine to minerals at deep mantle conditions were almost same as upper mantle conditions.

These results indicate that chlorine would not have partitioned into the core and deep mantle during planetary differentiation. In addition, given that the Cl/K and Cl/Zn ratios of the Earth is lower than any types of chondrites, the selective loss of chlorine from a magma ocean is required. Because the fluid-melt partition coefficient of chlorine at low-pressure conditions is generally above the unity, chlorine would have partitioned into a steam atmosphere over a magma ocean. If this is the case, the loss of primordial

atmosphere and ocean is the most likely scenario for explaining terrestrial missing chlorine. Our results show that chlorine depletion on Earth may be used as a geochemical tracer for understanding the loss of primordial Earth's atmosphere and ocean.

Appendices.

A. X-ray maps of the typical quenching run product for metal-silicate partitioning experiments.

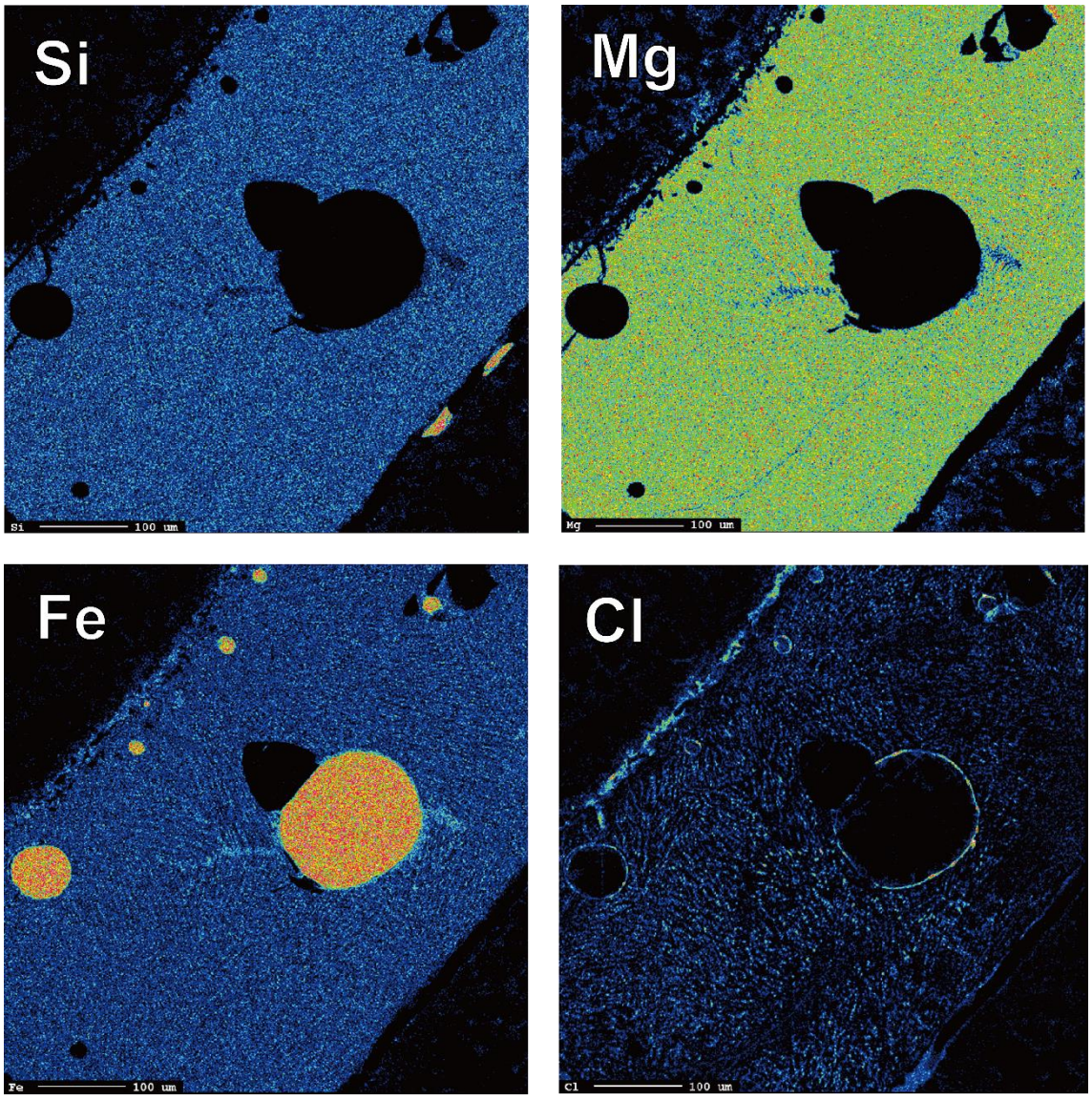

B. X-ray diffraction patterns of wadsleyite. The solid color lines indicate the reference for comparison.

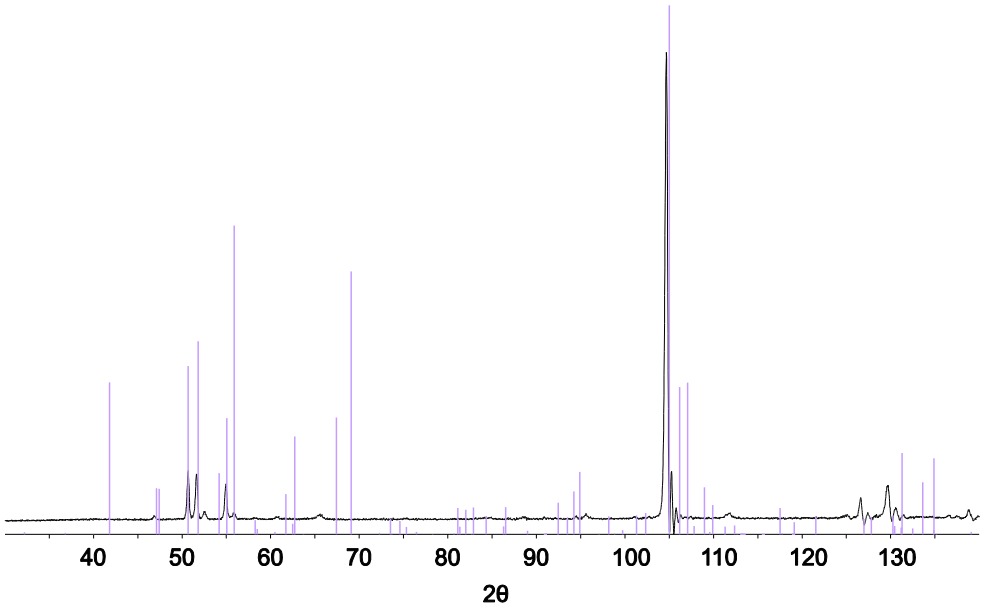

C. X-ray diffraction patterns of bridgmanite. The solid color lines indicate the reference for comparison.

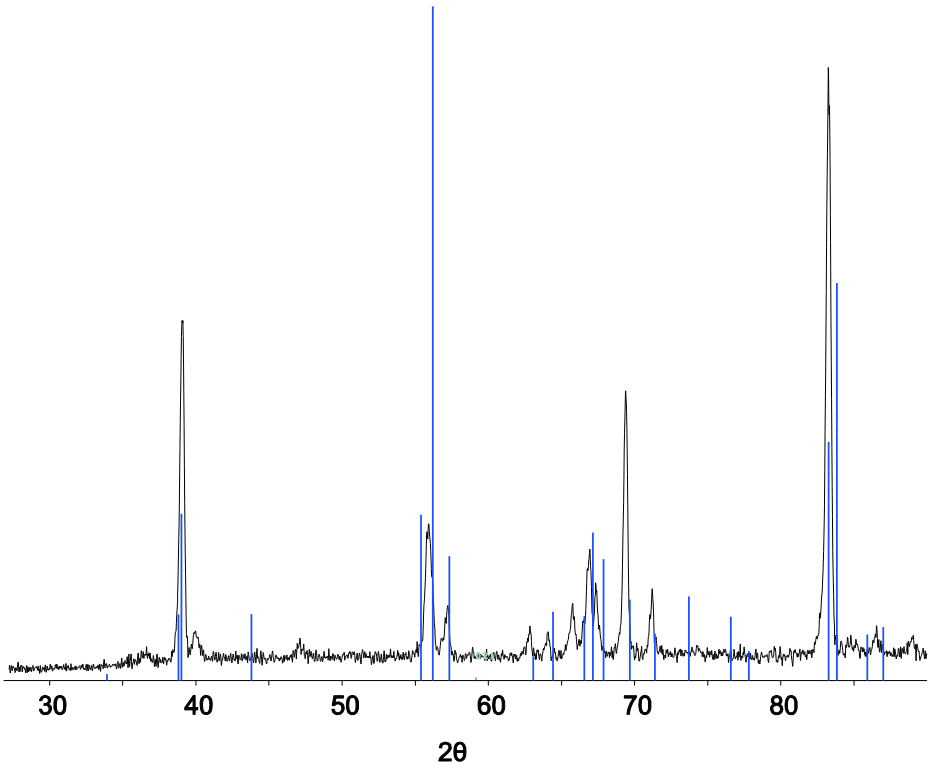

References

Abe, Y., Matsui, T., 1985. The formation of an impact-generated H_2O atmosphere and its implications for the early thermal history of the Earth. *J. Geophys. Res.* 90, C545-C549.

Aiuppa, A., 2009. Degassing of halogens from basaltic volcanism: Insights from volcanic gas observations. *Chem. Geol.* 263, 99-109.

Albarède, F., 2009. Volatile accretion history of the terrestrial planets and dynamic implications. *Nature* 461, 1227-1233.

Alexander, C. M. O'D., Bowden, R., Fogel, M. L., Howard, K. T., Herd, C. D. K., Nittler, L. R., 2012. The provenances of asteroid, and their contributions to the volatile inventories of the terrestrial planets. *Science* 337, 721-723.

Anders, E., Owen, T., 1977. Mars and Earth: Origin and Abundance of Volatiles. *Science* 198, 453-465.

Armytage, R. M. G., Jephcoat, A. P., Bouhifd, M. A., Porcelli, D., 2013. Metal-silicate partitioning of iodine at high pressures and temperatures: Implications for the Earth's core and ^{129}*Xe budgets. *Earth Planet. Sci. Lett.*, 373, 140-149.

Asphaug, E., Reufer, A., 2014. Mercury and other iro-rich planetary bodies as relics of inefficient accretion. *Nat. Geosci.* 7, 564-568.

Beattie, P., 1993. On the occurrence of apparent non-Henry's Law behavior in experimental partitioning studies. *Geochem. Cosmochim. Acta* 57, 47-55.

Bolfan-Casanova, N., Keppler, H., Rubie, D. C., 2003. Water partitioning at 660 km depth and evidence for very low water solubility in magnesium silicate perovskite. *Geophys. Res. Lett.* 30, 1905.

Bonsor, A., Leinhardt, Z. M., Carter, P. J., Elliott, T., Walter, M. J., Stewart, S. T., 2015. A collisional origin to Earth's non-chondritic composition? *Icarus* 247, 291-300.

Bouhifd, M. A., Gautron, L., Bolfan-Casanova, N., Malavergne, V., Hammouda, T., Andrault, D., Jephcoat, A. P., 2007. Potassium partitioning into molten iron alloys at high-pressure: Implications for Earth's core. *Geochem. Cosmochim. Acta* 160, 22-23.

Boujibar, A., Andrault, D., Bouhifd, M. A., Bolfan-Casanova, N., Devidal, J-L., Trcera, N., 2014. Metal-silicate partitioning of Sulphur, new experimental and thermodynamic constraints on planetary accretion. *Earth Planet. Sci. Lett.*, 391, 42-54.

Boujibar, A., Andrault, D., Bolfan-Casanova, N., Bouhifd, M. A., Monteux, J., 2015. Cosmochemical fractionation by collisional erosion during the Earth's accretion. *Nat. Commun.* 6.

Boyce, J. W., Treiman, A. H., Guan, Y., Ma, C., Eiler, J. M., Gross, J., Greenwood, J. P., Stolper, E. M., 2015. The chlorine isotope fingerprint of the lunar magma ocean. *Sci. Adv.* 1, e1500380.

Broadhurst, C. L., Drake, M. J., Hagee, B. E., Bernatowicz, T. J., 1992. Solubility and partitioning of Ne, Ar, Kr, and Xe in minerals and synthetic basaltic melts. *Geochem. Cosmochim. Acta* 56, 709-723.

Brown, H., 1949. Rare gases and the formation of the Earth'S atmosphere. In: Kuiper, G. (Ed.), The Atmosphere of the Earth and Planets. Univ. Chicago Press, Chicago, 258-266.

Campbell, I. H., O'Neill, H. S. C., 2012. Evidence against a chondritic Earth. *Nature* 483, 553-558.

Cartier, C., Hammouda, T., Boyet, M., Bouhifd, M. A., Devidal, J. –L., 2014. Redox control of the fractionation of niobium and tantalum during planetary accretion and core formation. *Nat. Geosci.* 7, 573-576.

Chambers, J. E., Wetherill, G. W., Boss, A. P., 1996. The stability of multi-planet systems.

Icarus 119, 261-268.

Chambers, J. E., Wetherill, G. W., 1998. Making the terrestrial planets: *n*-body integrations of planetary embryos in three dimensions. *Icarus* 136, 304-327.

Chi, H., Dasgupta, R., Duncan, M. S., Shimizu, N., 2014. Partitioning of carbon between Fe-rich alloy melt and silicate in a magma ocean – Implications for the abundance and origin of volatiles in Earth, Mars, and the Moon. *Geochem. Cosmochim. Acta* 139, 447-471.

Chou, C. L., 1978. Fractionation of siderophile elements in the earth's upper mantle. *Proc. Lunar planet. Sci. Conf*. 9, 219-230.

Dahl, T. W., Stevenson, D. J., 2010. Turbulent mixing of metal and silicate during planet accretion - and interpretation of the Hf-W chronometer. *Earth Planet. Sci. Lett*., 295, 177-186.

Dale, C. W., Burton, K. W., Greenwood, R. C., Gannoun, A., Wade, J., Wood, B. J., Pearson, D. G., 2012. Late accretion on the earliest planetesimals revealed by the highly siderophile elements. *Science* 336, 72-75.

Dalou, C., Koga, K., Shimizu, N., Boulon, J., Devida, J., 2012. Experimental determination of F and Cl partitioning between lherzolite and basaltic melt. *Contrib. Mineral. Petrol*. 151, 651-664.

Dasgupta, R., Walker, D., 2008. Carbon solubility in core melts in a shallow magma ocean environment and distribution of carbon between the Earth's core and the mantle. *Geochem. Cosmochim. Acta* 72, 4627-4641.

Dasgupta, R., Chi, H., Shimizu, N., Buono, A. S., Walker, D., 2013. Carbon solution and partitioning between metallic and silicate melts in a shallow magma ocean: Implications for the origin and distribution of terrestrial carbon. *Geochem. Cosmochim.*

Acta 102, 191-212.

Dauphas, N., Morbidelli, A., 2014. Geochemical and planetary dynamical views on the origin of Earth's atmosphere and oceans. Farquhar, J., (Ed.), Treatise on Geochemistry. The Atmosphere: History (second ed., vol. 6), Elsevier, Amsterdam, 1-35.

Day, J. M. D., Pearson, D. G., Tayler, L. A., 2007. Highly siderophile element constraints on accretion and differentiation of the Earth-Moon system. *Science* 315, 217-219.

Day, J. M. D., Walker, R. J., Qin, L., Rumble III, D., 2012. Late accretion as a natural consequence of planetary growth. *Nat*. *Geosci*. 5, 614-617.

de Niem, D., Kuhrt, E., Morbidelli, A., Motschmann, U., 2012. Atmospheric erosion and replenishment induced by impacts upon the Earth and Mars during a heavy bombardment. *Icarus* 221, 495-507.

Fabbrizio, A., Stalder, R., Hametner, K., Günther, D., 2013a. Experimental chlorine partitioning between forsterite, enstatite and aqueous fluid at upper mantle conditions. *Geochem*. *Cosmochim*. *Acta* 121, 684-700.

Fabbrizio, A., Stalder, R., Hametner, K., Günther, D., Marquardt, K., 2013b. Experimental partitioning of halogens and other trace elements between olivine, pyroxenes, amphibole and aqueous fluid at 2 GPa and 900-1,300 °C. *Contrib*. *Mineral*. *Petrol*. 166, 639-653.

Filiberto, J., Treiman, A. H., 2009. The effect of chlorine on the liquidus of basalt: First results and implications for basalt genesis on Mars and Earth. *Chem*. *Geol*., 263, 60-68.

Filiberto, J., Treiman, A. H., Giesting, P. A., Goodrich, C. A., Gross, J., 2014. High-temperature chlorine-rich fluid in the martian crust: A precursor to habitability. *Earth Planet*. *Sci*. *Lett*. 401, 110-115.

Frost, D. J., Mann, U., Asahara, Y., Rubie, D. C., 2008. The redox state of the mantle during and just after core formation. *Philos. Trans. R. Soc. A* 366, 4315-4337.

Genda, H., Abe, Y., 2003. Survival of a proto-atmosphere through the stage of giant impacts: the mechanical aspects. *Icarus* 164, 149-162.

Genda, H., Abe, Y., 2005. Enhanced atmospheric loss on protoplanets at the giant impact phase in the presence of oceans. *Nature* 433, 842-844.

Halliday, A. N., 2004. Mixing, volatile loss and compositional change during impact-driven accretion of the Earth. *Nature* 427, 505-509.

Halliday, A. N., 2013. The origins of volatiles in the terrestrial planets. *Geochim. Cosmochim. Acta* 105, 146-171.

Hamano, K., Abe, Y., 2010. Atmospheric loss and supply by an impact-induced vapor cloud: Its dependence on atmospheric pressure on a planet. *Earth Planets Space* 62, 599-610.

Hamano, K., Abe, Y., Genda, H., 2013. Emergence of two types of terrestrial planet on solidification of magma ocean. *Nature* 497, 607-610.

Hauri, E. H., Gaetani, G. A., Green, T. H., 2006. Partitioning of water during melting of the Earth's upper mantle at H_2O-unsaturated conditions. *Earth Planet. Sci. Lett.* 248, 715-734.

Hayashi, C., Nakazawa, K., Mizuno, H., 1979. Earth's melting due to the blanketing effect of the primordial dense atmosphere. *Earth Planet. Sci. Lett.* 43, 22-28.

Holzheid, A., Palme, H., Chakraborty, S., 1997. The activities of NiO, CoO and FeO in silicate melts. *Chem. Geol.* 139, 21-38.

Hirschmann, M. M., Dasgupta, R., 2009. The H/C ratios of Earth's near-surface and deep reservoirs, and consequences for deep Earth volatile cycles. *Chem. Geol.* 262, 4-16.

Hirschmann, M. M., 2016. Constraints on the early delivery and fractionation of Earth's major volatiles from C/H, C/N, and C/S ratios. *American Mineralogist* 101, 540-553.

Inoue, T., Wada, T., Sasaki, R., Yurimoto, H., 2010. Water partitioning in the Earth's mantle. *Phys. Earth Planet. Inter.* 183, 245-251.

Javoy, M., 1998. The birth of the Earth's atmosphere: the behaviour and fate of its major elements. *Chem. Geol.* 147, 11-25.

Kasting, J. F., Pollack, J. B., 1983. Loss of water from Venus. I. Hydrodynamic escape of hydrogen. *Icarus* 53, 479-508.

Kimura, K., Lewis, R. S., Anders, E., 1974. Distribution of gold and rhenium between nickel-iron and silicate melts: implications for the abundance of siderophile elements of the Earth and Moon. *Geochim. Cosmochim. Acta* 38, 683-701.

Kuramoto, K., Matsui, T., 1996. Partitioning of H and C between the mantle and core during the core formation in the Earth: Its implications for the atmospheric evolution and redox state of early mantle. *J. Geophys. Res.* 101, 14909-14932.

Kuwahara, H., Gotou, H., Ogawa, N., Yamaguchi, A., Ishibashi, K., Yagi, T., Sugita, S., 2015. Metal-silicate partitioning of chlorine: Implications for terrestrial missing chlorine. *Goldschmidt Abstracts* 2015, 1730.

Lebrun, T., Massol, H., Chassefière, E., Davaille, A., Marcq, E., Sarda, P., Leblanc, F., Brandeis, G., 2013. Thermal evolution of an early magma ocean in interaction with the atmosphere. *J. Geophys. Res.* 118, 1-22.

Li, J., Agee, C. B., 1996. Geochemistry of mantle-core differentiation at high pressure. *Nature* 381, 686-689.

Li, Y., Wiedenbeck, M., Shcheka, S., Keppler, H., 2013. Nitrogen solubility in upper mantle minerals. *Earth Planet. Sci. Lett.*, 377-378, 311-323.

Liebske, C., Corgne, A., Frost, D. J., Rubie, D. C., Wood, B. J., 2005. Compositional effects on element partitioning between Mg-silicate perovskite and silicate melts. *Contrib. Mineral. Petrol.* 149, 113-128.

Litasov, K., Ohtani, E., Langenhorst, F., Yurimoto, H., Kubo, K., Kondo, T., 2003. Water solubility in Mg-perobskites and water shortage capacity in the lower mantle. *Earth Planet. Sci. Lett.* 211, 189-203.

Litasov, K., 2012. The influence of Al_2O_3 on the H_2O content in periclase and ferropericlase at 25 GPa. *Russian Geology and Geophysics* 51, 644-649.

Lodders, K., 2000. An oxygen isotope mixing model for the accretion and composition of rocky planets. *Space Sci. Rev.* 92, 341-354.

Lodders, K., 2003. Solar system abundances and condensation temperatures of the elements. *Astrophys. J.* 591, 1220-1247.

Marty, B., 2012. The origins and concentrations of water, carbon, nitrogen, and noble gases on Earth. *Earth Planet. Sci. Lett.* 313-314, 56-66.

Matsui, T., Abe, Y., 1986a. Evolution of an impact-induced atmosphere and magma ocean on the accreting Earth. *Nature* 319, 303-305.

Matsui, T., Abe, Y., 1986b. Impact-induced atmospheres and oceans on Earth and Venus. *Nature* 322, 526-528.

McDonough, W. F., Sun, S-S., 1995. The composition of the Earth. *Chem. Geol.* 120, 223-253.

McDonough, W. F., 2003. Compositional model for the Earth's core. Carison, R. W. (Ed.), The Mantle and Core, Treatise on Geochemistry 2, Elsevier-Pergamon, Oxford, 547-568.

Melosh, H. J., Vickery, A. M., 1989. Impact erosion of the primordial atmosphere on Mars. *Nature* 338, 487-489.

Métrich, N., Bertagnini, A., Landi, P., Rosi, M., 2001. Crystallization driven by decompression and water loss at Stromboli volcano (Aeolian islands, Italy). *Journal of Peterology* 42, 1471-1490.

Mungall, J. E., Brenan, J. M., 2003. Experimental evidence for the chalcophile ehavior of the halogens. *Can*. *Mineral*. 41, 207-220.

Murakami, M., Hirose, K., Yurimoto, H., Nakashima, S., Takafuji, N., 2002. Water in Earth's lower mantle. *Science* 295, 1885-1887.

Nakajima, M., Stevenson, D. J., 2015. Melting and mixing states of the Earth's mantle after the Moon-forming impact. *Icarus* 427, 286-295.

Nimmo, F., Agnor, C. B., 2006. Isotopic outcomes of *N*-body accretion simulations: constraints on equilibration processes during large impacts from Hf/W observations. *Earth Planet*. *Sci*. *Lett*., 243, 26-43

Nimmo, F., O'Brien, D. P., Kleine, T., 2010. Tungsten isotopic evolution during late-stage accretion: constraints on Earth-Moon equilibration. *Earth Planet*. *Sci*. *Lett*., 292, 363-370.

O'Brien, D. P., Walsh, K. J., Morbidelli, A., Raymond, S. N., Mandell, A. M., 2014. Water delivery and giant impacts in the 'Grand Tack' scenario. *Icarus* 239, 74-84.

Okuchi, T., 1997. Hydrogen partitioning into molten iron at high pressure: Implications for Earth's core. *Science* 278, 1781-1784.

O'Neill, H. S. C., Palme, H., 2008. Collisional erosion and the non-chondritic composition of the terrestrial planets. *Philos*. *Trans*. *R*. *Soc*. *A* 366, 4205-4238.

Pearson, D. G., Brenker, F. E., Nestola, F., McNeill, J., Nasdala, L., Hutchison, M. T., Matveev, S., Mather, K., Silversmit, G., Schmitz, S., Vekemans, B., Vincze, L., 2014. Hydrous mantle transition zone indicated by ringwoodite included within diamond. *Nature* 507, 221-224.

Pepin, R. O., 1991. On the origin and early evolution of terrestrial planet atmospheres and meteoritic volatiles. *Icarus* 92, 2-79.

Pepin, R. O., 1992. Origin of noble gases in the terrestrial planets. *Annu. Rev. Planet. Sci.* 20, 389-430.

Pepin, R. O., Porcelli, D., 2002. Origin of noble gases in the terrestrial planets. *Rev. Mineral. Geochem.* 47, 191-246.

Pujol, M., Marty, B., Burgess, 2011. Chondritic-like xenon trapped in Archean rocks: A possible signature of the ancient atmosphere. *Earth Planet. Sci. Lett.*, 308, 298-306.

Raymond, S. N., Quinn, T., Lunine, J. I., 2004. Making other earths: dynamical simulations of terrestrial planet formation and water delivery. *Icarus* 168, 1-17.

Raymond, S. N., Quinn, T., Lunine, J. I., 2005. The formation and habitability of terrestrial planets in the presence of close-in giant planets. *Icarus* 177, 256-263.

Ringwood, A. E., 1966. Chemical evolution of the terrestrial planets. *Geochim. Cosmochim. Acta* 30, 41-104.

Roberge, M., Bureau, H., Bolfan-Casanova, N., Frost, D., Raepsaet, C., Surble, S., Khodja, H., Fiquet, G., 2013. F and Cl solubilities in wadsleyite and ringwoodite. *Mineralogical Magazine* 77(5). 2068.

Roberge, M., Bureau, H., Bolfan-Casanova, N., Frost, D. J., Raepsaet, C., Surble, S., Khodja, H., Auzende, A., Fiquet, G., 2015. Is the transition zone a deep reservoir for fluorine? *Earth Planet. Sci. Lett.* 429, 25-32.

Rose-Weston, L., Brenan, J. M., Fei, Y., Secco, R. A., Frost, D. J., 2009. Effect of pressure, temperature, and oxygen fugacity on the metal-silicate partitioning of Te, Se, and S: Implications for earth differentiation. *Geochim. Cosmochim. Acta* 73, 4598-4615.

Roskosz, M., Bouhifd, M. A., Jephcoat, A. P., Marty, B., Mysen, B. O., 2013. Nitrogen solubility in molten metal and silicate at high pressure and temperature. *Geochim. Cosmochim. Acta* 121, 15-28.

Rubie, D. C., Frost, D. J., Mann, U., Asahara, Y., Nimmo, F., Tsuno, K., Kegler, P., Holzheid, A., Palme, H., 2011. Heterogeneous accretion, composition and core-mantle differentiation of the Earth. *Earth Planet. Sci. Lett.*, 301, 31-42.

Rubie, D. C., Jacobson, S. A., Morbidelli, A., O'Brien, D. P., Young, E. D., de Vries, J., Nimmo, F., Palme, H., Frost, D. J., 2015. Accretion and differentiation of the terrestrial planets with implications for the compositions of early-formed solar system bodies and accretion of water. *Icarus* 248, 89-108.

Rudge, J. F., Kleine, T., Bourdon, B., 2010. Broad bounds on Earth's accretion and core formation constrained by geochemical models. *Nat. Geosci.* 3, 49-443.

Savage, P. S., Moynier, F., Chen, H., Shofner, G., Siebert, J., Badro, J., Puchtel, I. S., 2015. Copper isotope evidence for large-scale sulphide fractionation during Earth's differentiation. *Geochem. Persp. Let.* 1, 53-64.

Schaefer, L., Fegley Jr., B., 2007. Outgassing of ordinary chondritic material and some of its implications for the chemistry of asteroids, planets, and satellites. *Icarus* 186, 462-483.

Schlichting, H. E., Sari, R., Yalinewich, A., 2015. Atmopsheric mass loss during planet formation: The importance of planetesimal impacts. *Icarus* 247, 81-94.

Sharp, Z. D., Barnes, J. D., Brearley, A. J., Chaussidon, M., Fischer, T. P., Kamenetsky, V. S., 2007. Chlorine isotope homogeneity of the mantle, crust and carbonaceous chondrites. *Nature* 446, 1062-1065.

Sharp, Z. D., Draper, D. S., 2013. The chlorine abundance of Earth: Implications for a habitable planet. *Earth Planet*. *Sci*. *Lett*., 369-370, 71-77.

Shcheka, S. S., Keppler, H., 2012. The origin of the terrestrial noble-gas signature. *Nature* 490, 531-534.

Shuvalov, V., 2009. Atmopsheric erosion iduced by obique impacts. *Meteorit*. *Planet*. *Sci*. 44, 1095-1105.

Siebert, J., Corgne, A., Ryerson, F. J., 2011. Systematics of metal-silicate partitioning for many siderophile elements applied to Earth's core formation. *Geochem*. *Cosmochim*. *Acta* 75, 1451-1489.

Siebert, J., Badro, J., Antonangeli, D., Ryerson, F. J., 2012. *Earth Planet*. *Sci*. *Lett*., 321-322, 189-197.

Signorelli, S., Carroll, M. R., 2000. Solubility and fluid-melt partitioning of Cl in hydrous phonolitic melts. *Geochem*. *Cosmochim*. *Acta* 64, 2851-2862.

Signorelli, S., Carroll, M. R., 2002. Experimental study of Cl solubility in hydrous alkaline melts: constraints on the theoretical maximum amount of Cl in trachytic and phonolitic melts. *Contrib*. *Miner*. *Petrol*., 143, 209-218.

Straub, S. M., Layne, G. D., 2003. The systematics of chlorine, fluorine, and water in Izu arc front volcanic rocks: Implications for volatile recycling in subduction zones *Geochim*. *Cosmochim*. *Acta* 67, 4179-4203.

Tolstikhin, I., O'Nions, R. K., 1994. The Earth's missing xenon: A combination of early degassing and of rare gas loss from the atmosphere. *Chem*. *Geol*. 115, 1-6.

Tonks, W. B., Melosh, H. J., 1992. Core formation by giant impacts. *Icarus* 100, 326-346.

Tonks, W. B., Melosh, H. J., 1993. Magma ocean formation due to giant impacts. *J. Geophys. Res.* 98, 5319-5333.

Thibault, Y., Walter, M. J., 1995. The influence of pressure and temperature on the metal-silicate partition coefficients of nickel and cobalt in a model C1 chondrite and implications for metal segregation in a deep magma ocean. *Geochem. Cosmochim. Acta* 59, 991-1002.

Tucker, J. M., Mukhopadhyay, S., 2014. Evidence for multiple magma ocean outgassing and atmospheric loss episodes from mantle noble gases. *Earth Planet. Sci. Lett.*, 393, 254-265.

Wade, J., Wood, B. J., 2005. Core formation and the oxidation state of the Earth. *Earth Planet. Sci. Lett.*, 236, 78-95.

Wade, J., Wood, B. J., Tuff, J., 2012. Metal-silicate partitioning of Mo and W at high pressures and temperatures: Evidence for late accretion of sulphur to the Earth. *Geochem. Cosmochim. Acta* 85, 58-74.

Walker, D., Norby, L., Jones, J. H., 1993. Superheating effects on metal-silicate partitioning of siderophile elements. *Science* 262, 1858-1861.

Wang, Z., Becker, H., 2013. Ratios of S, Se, and Te in the silicate Earth require a volatile-rich late veneer. *Nature* 499, 328-332.

Wanke, H., Dreibus, G., 1988. Chemical composition and accretion history of terrestrial planets. *Philos. Trans. R. Soc. A* 325, 545-557.

Wasson, J. T., Kalleymeyn, G. W., 1988. Compositions of chondrites. *Philos. Trans. R. Soc. London* A325, 535-544.

Wood, B. J., 1993. Carbon in the core. *Earth Planet. Sci. Lett.*, 117, 593-607.

Wood, B. J., Walter, M. J., Wade, J., 2006. Accretion of the Earth and segregation of its core. *Nature* 441, 825-833.

Wood, B. J., Halliday, A. N., 2010. The lead isotopic age of the Earth can be explained by core formation alone. *Nature* 465, 767-771.

Wood, B. J., Kiseeva, E. S., Mirolo, F. J., 2014. Accretion and core formation: The effect of sulfur on metal-silicate partition coefficients. *Geochem*. *Cosmochim*. *Acta* 145, 248-267.